

Manuscript Number: PROTEC-D-13-00551R2

Title: Physico-chemical Behaviour of Polyether Ketone (PEK) in High Temperature Laser Sintering

Article Type: Research Paper

Keywords: Polyether Ketone, selective laser sintering, high temperature

Corresponding Author: Dr. Oana Ghita,

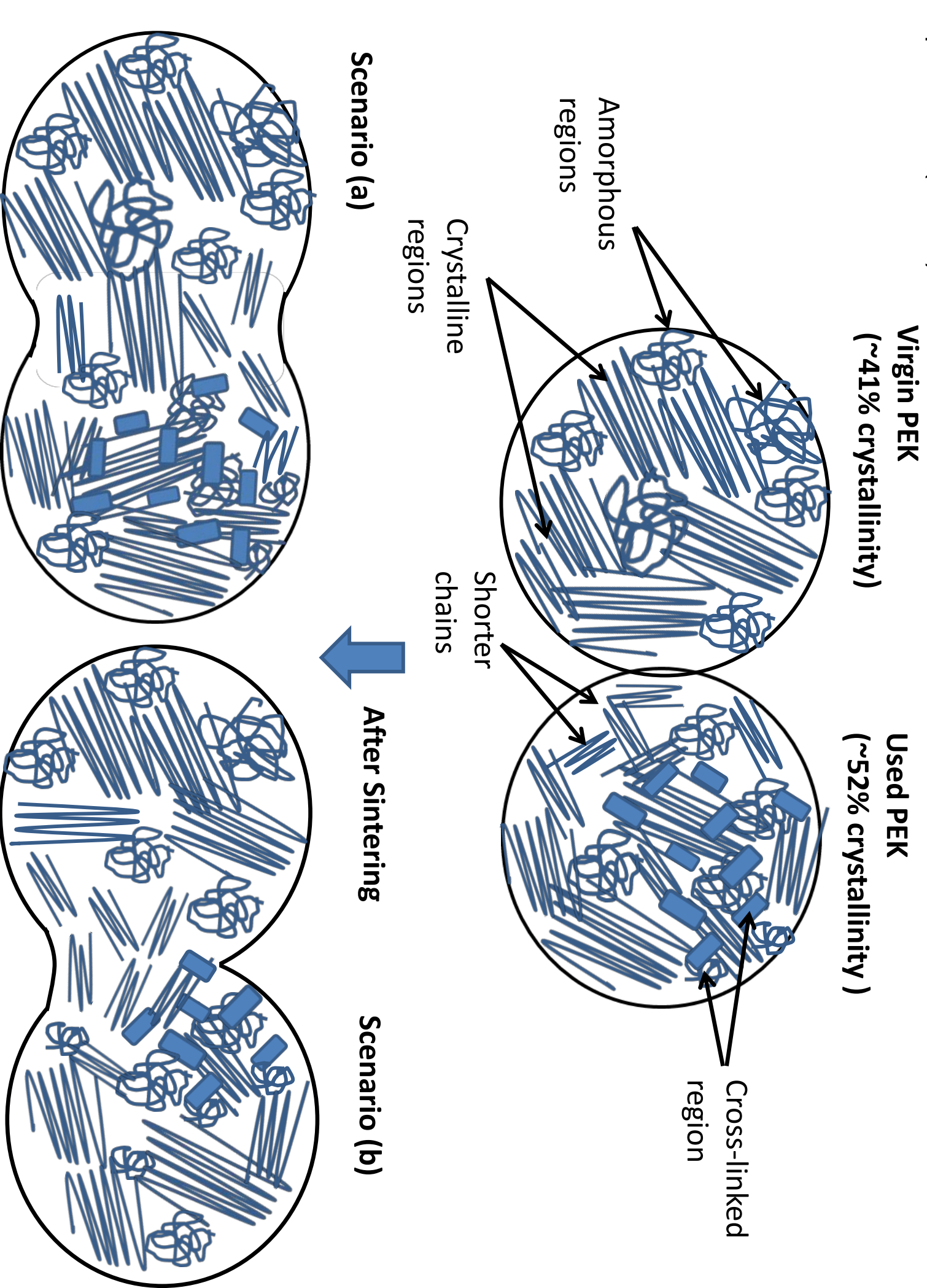
Corresponding Author's Institution: Univeristy of Exeter

First Author: Oana Ghita

Order of Authors: Oana Ghita; Edward James; Rachel Trimble; Ken E Evans

Abstract: Laser sintering (LS) of polymers has high potential for growth as a manufacturing technique into a wide range of applications provided the range of engineering polymers available for LS expands and machines and SLS process conditions are optimised for such materials.

This study is the first investigation into laser sintering of both virgin and used polyether ketone PEK powder using a bespoke high temperature polymer laser sintering machine (EOS P800). The physico-chemical results reveal that, in spite of polymer degradation, used PEK has a viable processing window for LS manufacturing which, combined with optimisation of specific parameters can successfully lead to manufacture of good quality parts. The proposed sintering mechanism of both, virgin and used powders is supported by the experimental data. The incorporation of 30 % used HP3 PEK powder led to an approximately 17% drop in tensile strength.



Highlights:

- First investigation into laser sintering of virgin and used polyether ketones (PEK) using a bespoke high temperature selective laser sintering system
- The incorporation of 30 % used PEK powder led to an approximately 17% drop in tensile strength
- The use of a higher laser power improves the surface finish but it doesn't affect the porosity and mechanical strength of the parts incorporating reused powder
- The used PEK powder suffers degradation which affects the particle coalescence process

Physico-chemical Behaviour of Polyether Ketone (PEK) in High Temperature Laser Sintering

O. Ghita^{1*}, E. James², R. Trimble¹, K. E. Evans¹

¹*University of Exeter, College of Engineering, Mathematics and Physical Sciences,
North Park Road, EX4 4QF, UK*

²*Centre for Additive Layer Manufacturing (CALM), University of Exeter, College of
Engineering, Mathematics and Physical Sciences, North Park Road, EX4 4QF, UK*

Abstract

Laser sintering (LS) of polymers has high potential for growth as a manufacturing technique into a wide range of applications provided the range of engineering polymers available for LS expands and machines and LS process conditions are optimised for such materials.

This study is the first investigation into laser sintering of both virgin and used polyether ketone PEK powder using a bespoke high temperature (HT) polymer laser sintering machine (known commercially as EOSINT P800). The physico-chemical results reveal that, in spite of polymer degradation, used PEK has a viable processing window for LS manufacturing which, combined with optimisation of specific parameters can successfully lead to manufacture of good quality parts. The proposed sintering mechanism of both, virgin and used powders is supported by the experimental data. The incorporation of 30 % used HP3 PEK powder led to an approximately 17% drop in tensile strength.

Keywords: Polyether Ketone, selective laser sintering, high temperature

*Corresponding author information: Tel: +44 (0)1392 263667

Fax: +44 (0)1392 263616

E-mail address: O.ghita@exeter.ac.uk (O.R. Ghita)

1. Introduction

Laser Sintering is an additive manufacturing technique that builds fully functional components layer-by-layer from particulate materials. Consolation of the powder is achieved through a laser selectively sintering areas of the powder bed.

Although LS is of great interest to various manufacturing sectors (e.g. aerospace, automotive, medical) and is increasingly investigated as an innovative and unique manufacturing process due to its design freedom and complex geometries, there is a limited number of polymeric materials currently available for LS use and those used lack mechanical performance, a key requirement for most applications.

Most efforts in improving polymeric laser sintered parts properties have focused on reinforcing standard polyamide (PA) matrices with glass beads, carbon and aluminium. For example, Kumar and Kruth (2010) presented a comprehensive review of composite PA based materials developed for additive manufacturing. However, the matrix intrinsic characteristics such as low melting temperatures (T_m) and low glass transition temperatures (T_g) still limit the range of applications of these materials.

The possibility of using thermoplastics in the polyaryletherketone family combined with the benefits offered by the AM process could lead to an increased uptake of the

technology by industry. The high melting temperatures, excellent mechanical properties, high wear and chemical resistance, along with high resistance to burning, smoke and toxicity performance, enabled thermoplastics such as PEK and polyether ether ketone (PEEK) to be used along the years, using standard manufacturing techniques such as injection moulding, compression moulding or rotomoulding, across various industrial sectors (automotive, aerospace and medical) . Applications range from piston components, bearing linings, cable couplings and connections, through to prosthetic and pump casings.

Rechtenwald et al. (2005), attempted to adapt the standard PA laser sintering equipment for use of high temperature thermoplastics such as PEEK. One of the main challenges was achieving and maintaining a much higher preheating temperature than is required for standard polyamine 12 (PA12) processing. The authors, modified an EOSINT P380 laser sintering machine by integrating a circular building platform and an additional heating device to enable pre-heating at higher temperatures, 250°C. The tested samples were adversely affected by this low preheating temperature. Using the same system, Schmidt et al. (2007), noticed that the process boundaries (energy input and the preheating temperature) affect the relative density of the parts which strongly influenced the bending test results. The porosity was varied from zero to 15%.

In a subsequent study by Pohle et al. (2007), the same research group tried to improve the design by adding a “high-temperature inner process chamber” called the “Heating Dome” to the standard PA12 equipment. These modifications allowed the pre-heating temperature to be further increased to 345°C, the melting temperature of PEEK being approximately 370°C. Using this system the preheating

was uniform over the entire building platform. Unfortunately no mechanical testing was carried out, the study being primarily focused on designing medical implants (based on PEEK and β - tri-calcium phosphate (TCP)) and evaluation of their biological behaviour.

Tan et al. (2003), attempted the use of PEEK/hydroxyapatite (HA) blends for tissue engineering applications using a powder bed rapid prototyping technique. Initially the investigation focused on defining the optimum combination of laser power and bed temperature for sintering. SEM images of the PEEK/HA parts were presented but no further investigations carried out.

In addition to the preheating temperature difficulty, Pohle et al. (2007), have raised concerns that the morphology of PEEK is highly irregular and it does not flow smoothly. Pohle et al. (2007) tried to overcome this issue by introducing 1% carbon black in addition to other bioactive ingredients. In all cases, the repose angle was reduced from 41° to 27° and the flow ability improved.

A recent study by Beard et al. (2011) used the first bespoke high temperature standard SLS machine (EOS P800) to manufacture PEK parts. This is the first study to use PEK, all previous studies using PEEK polymer on modified systems. Although PEEK and PEK are members of the same polyaryletherketone family, the difference in chemical structure (see Figure 1) leads to a significantly higher melting temperatures and glass transition temperature for PEK ($T_m= 372^\circ\text{C}, T_g= 164^\circ\text{C}$) over PEEK ($T_m=343^\circ\text{C}, T_g=143^\circ\text{C}$) as per the datasheets provided by Victrex, (2013). PEEK was the preferred material of choice in all previous studies due to its lower melting and glass transition temperatures which allows easier implementation in modified nylon laser sintering systems and due to being more commonly used than PEK.

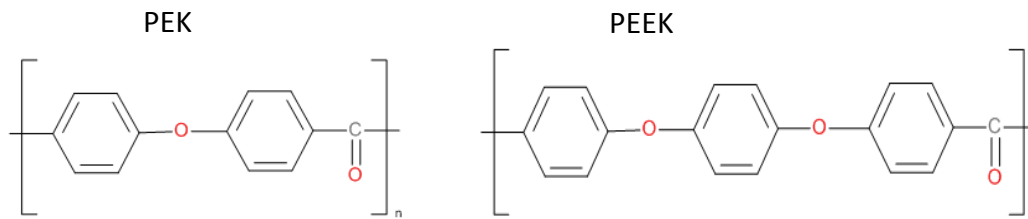


Figure 1 Chemical structure of PEK and PEEK

The study of Beard et al. (2011) is the only one to investigate use of PEK in SLS and to use a standard high temperature SLS machine to manufacture polymeric parts. The differential scanning calorimetry (DSC) and dynamic mechanical thermal analyser (DMTA) results showed good repeatability and consistency within the same sample and across a range of samples tested, low porosity and good bonding between layers.

Dotchev and Yusoff (2009) established that during SLS of nylon parts, the powder left un-sintered in the process suffers degradation, both time and temperature having a strong detrimental effect on the un-sintered powder properties. The authors, Dotchev and Yusoff (2009) noticed that the melt flow rate (MFR) index of fresh PA2200 powder decreased dramatically during the first 100h of continuous heating. Higher temperatures (150°C and above) which represent temperatures closer to the centre of the build can lead to a drop in MFR from 60 to 12-25g/10min.

These recycling studies were driven by economic factors such as the high cost of virgin material and the large volumes of scrap powder produced from build failures due to lack of repeatability and mechanically unsatisfactory parts. Dotchev and

Yusoff, (2009) determined that the cost of polyamide PA220 powder for a full build in the EOSINT P700 system costs approximately 4,700Euros (approx. £4,000) with 50% new and 50% used PA2200 powder. Currently, HP3 PEK powder material for a full build in the EOSINT P800 system costs approximately £50,000, ten times more expensive. Due to their unique characteristics and performance, materials within the PAEK family are very expensive, HT-LS PEK and PEEK powder grades being the most expensive powders available, currently not being reused. Therefore their ability to be reused is even more important and needs to be assessed. Due to the prohibitive cost of PEK in comparison with polyamide, there is high pressure on users and parts manufacturers to investigate the recycling of the HP3 PEK powder. In other industry sectors such as injection moulding, recycling of PEEK materials received a lot of attention. A recent study carried out by McLauchlin et al. (2013) showed that recycled PEEK retains its tensile properties through at least three moulding and regrinding cycles.

Dotchev and Yusoff, (2009) observed that the simple reuse of recycled powder with little or no addition of fresh powder leads to a rough surface finish known as “orange peel” and higher shrinkage.

Zarringhalam et al. (2006) noticed that the used powder has an increased molecular weight. When mixed with virgin powder, the blend leads to a higher elongation at break in the parts built while Young’s modulus and tensile strength exhibit very little change. Similarly, Gornet et al. (2002) noticed an increase in elongation at break when re-using nylon powder for seven consecutive builds but the tensile strength recorded a drop of approximately 25% between the 5th and 7th build.

Following on from the work of Beard et al. (2011), this study further analyses the properties of SLS PEK parts and also investigates the physico-chemical characteristics of virgin and used PEK powder within the SLS process. The work begins with analysis of virgin and used powder followed by mechanical and morphological investigation of PEK parts manufactured using virgin powder and virgin/used PEK powder blends at two specific laser powers: 15W; considered to be the standard parameter; and 16.5W. The results show that although the used PEK powder suffers degradation through cross-linking, the reuse of up to 30 % of PEK powder is possible with only 16% drop in tensile strength and elongation at break. The micro-CT results showed that the incorporation of used PEK powder leads to a higher porosity in the sintered parts, but a careful optimisation of the processing parameters can eliminate porosity and improve surface finish.

2. PEK Parts Manufacturing – Selective Laser Sintering

2.1 Materials

The virgin material used was EOS HP3 powder (EOS, 2012), supplied by EOS Systems Ltd. EOS HP3 is polyether ketone (PEK) powder specifically manufactured for use in additive manufacture.

The used HP3 powder used in the study was the unsintered HP3 PEK powder obtained at the end of a standard run in the EOSINT P800 laser sintering system. The used powder was sieved and blends of 80/20 and 70/30% virgin/used HP3 powders were mixed by weight.

2.2 Selective Laser Sintering process of P800

The HT laser sintering system (EOSINT P800) operates similar to a standard polyamide system (e.g. EOSINT P760 or Formiga P110) (EOS, 2013) and consists of two 50W CO₂ lasers, a recoating mechanism, a heated piston, infrared lamps focused on the powder bed and a heated exchangeable frame which gives a maximum build volume of 700 x 380 x 580mm.

The machine initially goes through a warm up stage where it gradually increases the temperature of the base powder to the 368°C process temperature and within an inert gas atmosphere. After completion of the warm up stage the machine starts the laser sintering build stage. During the laser sintering process the powder is applied to process bed by means of a recoating mechanism to give a layer thickness of 0.12mm. The part contours are scanned by the CO₂ lasers and subsequently filled to complete the cross sectional layer of the CAD data. Once sintered, the material goes through a post sintering stage where the powder layer is exposed to thermal radiation for a further 12seconds during which “the sintered powder grains finally flow to form a homogeneous molten film” (EOS, 2010). The energy applied during the standard sintering process may be insufficient to form a homogenous molten film with the material EOS PEEK HP3, hence the post sintering time at build temperature. The piston then drops by the layer thickness and the recoating mechanism applies the next layer of powder. On completion of the build the machine enters a cool down stage where it controls the cooling rate of the powder to room temperature. At room temperature the exchangeable frame is removed from the machine and the parts are cleaned of unused powder.

2.3 Parts Build Area

Due to the cost of materials, the EOSINT P800 system was run in a reduced build mode, which reduces the effective build area to 420 x 230 x 250mm as shown in Figure 2. The EOSINT P800 reduced build mode includes a controlled loading and coating path in conjunction with a volume reduction of the left dispensing container. Due to the temperatures used, the powder has the ability to self-support itself at the end of each layer by layer spreading stage without the need to introduce a support wall.

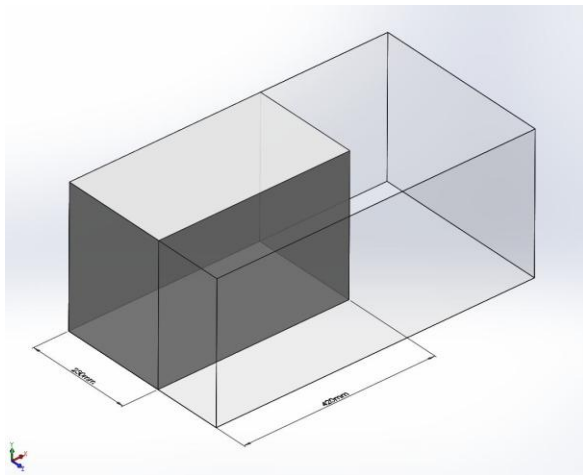


Figure 2 Reduced build diagram

Parts were built in the shape of dogbone geometries with the following dimensions (80 x 10 x 4 mm) according to ISO527-2 test specimen type 1BA.

The parts were built using two laser powers: 15W and 16.5W, and 2250mm/s scan speed. Eight dogbone parts were built at each laser power. The position of the parts in the build bed is shown in Figure 3.

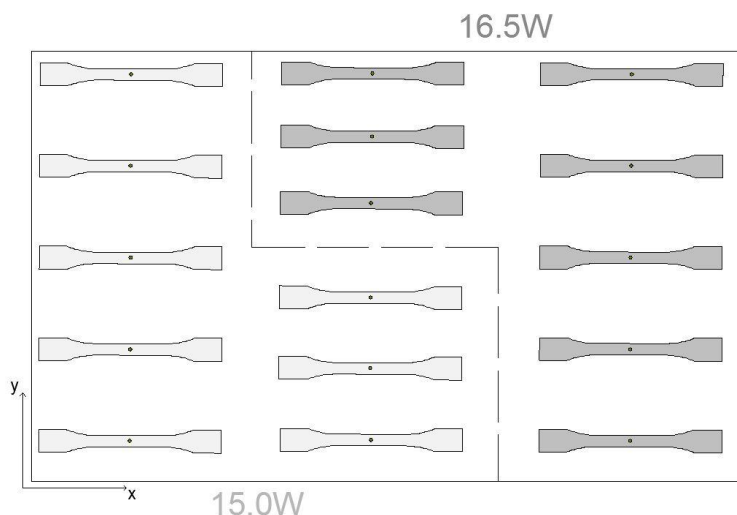


Figure 3 Diagram of the build

3. Experimental Methods

3.1 Particle Size Analysis

Particle size distribution was determined by light scattering analysis using a Micromeritics Saturn Digisizer 5200. The powder was dispersed in 6.7g sodium hexametaphosphate and 1.3g sodium hydrogen carbonate in 2 litres deionised water. Three repeats were taken for each sample.

3.2 Reduced viscosity measurements

0.25 g of polymer was treated overnight in concentrated sulphuric acid (25 mL, >95%, 1% w/v) to yield a bright orange polymer solution. Polymer solution viscometry was carried out in a water bath at 25 °C using a D-type Ubbelodhe tube. All samples were allowed 5 minutes to equilibrate to 25° C after pouring into the U-tube. Pure solvent and polymer solution samples were run to determine the time (t_0) and time (t) respectively, required for a specific volume to pass through the capillary

length. In all cases a minimum of three runs were undertaken, to an error of +/-0.2 second. An average of these results was used to determine the reduced viscosity.

3.3 Differential Scanning Calorimetry (DSC)

The DSC experiments were carried out using a Mettler-Toledo DSC 821e calorimeter under a nitrogen flow of 60 ml minute⁻¹ using dynamic scans at a heating rate of 10°C min⁻¹ from 30°C to 400°C for virgin powder and from 30 to 440°C for used powder. Six repeat cycles were performed on virgin and used HP3 powder. The degree of crystallinity is then given by dividing the heat of fusion of melting by the heat of fusion for 100% crystalline PEK. Blundell et al., 1983, determined the enthalpy of fusion for 100% crystalline PEK as 130J g⁻¹.

3.4 Mechanical Testing

Tensile testing was carried out using a LLOYD instruments EZ20 mechanical testing machine. Testing speed for all samples was 10mm/min breaking speed and gauge length 30mm. Eight samples were tested for each batch.

During initial trials it was noticed that many of the test specimens were breaking close to the clamps and not in the middle of the gauge length. Surface roughness and micro-cracks along the dogbone samples were the main reason for such behaviour. Thereafter, the parts were polished along the XZ surface of the dogbone (see Figure 4) to allow repeatable breaking towards the middle of the gauge length. All samples presented here were polished before performing mechanical testing.

3.5 Optical microscopy under hot stage

A small number of particles were spread on a glass slide which was mounted in a Linkam THMS600 microscope stage placed under a Bruker IRScope II in visual/reflectance mode connected also to a DinoEye eyepiece camera. Particles were heated to 440°C at 100°C/min and images were taken through the microscope at temperature intervals of 2°C during the experiment using DinoCapture 2.0 software.

3.6 Surface Topology Measurements

Surface topology measurements were made using a Taylor-Hobson Talyscan 150 surface profiler. Measurements were made using a laser probe with a deflection range of 6.29mm and a resolution of 162µm. The roughness parameter used, surface roughness (S_a), is a standard surface measurement calculated from the arithmetic mean of the deviations from the mean as described in the EUR 15 178 EN report (Stout et al., 1993). The TalyMap software was used to perform the analysis of the surface profile data.

Surface roughness measurements were carried out on the XY sides of the dogbones as shown in Figure 4. In each case the scanned area was 3 x 2mm.

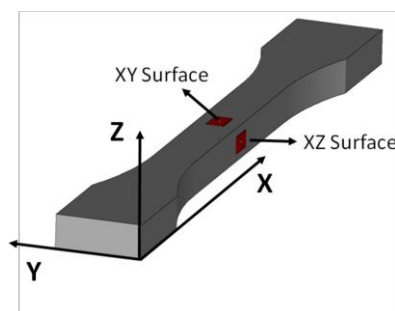


Figure 4 XY area used for surface roughness measurements

3.7. Micro Computer Tomography (μ CT)

Computer Tomography was performed using a CT 160 Xi System. The CT 160 Xi system is fitted with a high contrast x-ray image intensifier, 100KV 5 micron open type x-ray source to reconstruct the image. Global porosity value was measured in six tensile tests samples: 100% virgin PEK; 80/20% and 70/30% virgin/used HP3 PEK, each part manufactured by sintering at 15 and 16.5W laser power.

4. Results and Discussion

4.1 Particle Size Distribution

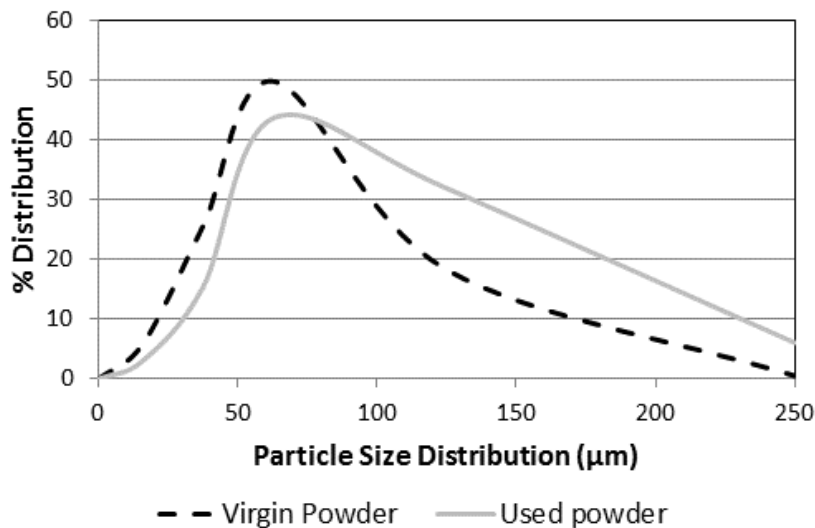


Figure 5 Particle size distribution of virgin and used HP3 PEK powder

As it can be seen in Figure 5, the used PEK powder presented a higher particle size distribution in comparison with virgin PEK powder. These findings are different from the results of Martinez et al. (2011), on aged InnovPA 1550 and XformPA, which

showed a slight decrease in used particle size in comparison with virgin powders. It is important to mention also that the analysis was qualitative rather than quantitative. It is well established by Shi et al. (2004), that deviation from the optimal particle size (75-150 μm) can lead to difficulties in powder flow ability (when particle size is too small) or increased roughness and porosity (when particles are too large). In this case, although there is a slight variation in distribution, the reuse of recovered HP3 powder is not expected to significantly affect the properties of the sintered parts.

4.2 Reduced viscosity measurements

The virgin PEK powder fully dissolved in the polymer solution and the reduced viscosity measured was 1.225. The used PEK did not dissolve well, produced a high level of “gels” (insolubles) and the measured reduced viscosity was 1.290. The increase in reduced viscosity combined with the presence of “gels” (insolubles), clearly indicate the presence of cross-linking sites in the used PEK.

4.3 Differential Scanning Calorimetry of HP3 PEK powders

The DSC results show an increase in crystallinity from 41.6 ± 3.9 % for virgin PEK to 52.1 ± 3.0 % for used PEK. Few studies have achieved an increase in crystallinity as high as this. For example, Cebe (1988) reports a 10% increase in crystallinity when annealing the samples at 319°C. The high degree of crystallinity achieved in used HP3 PEK is not surprising considering the slow heating and cooling time required for manufacturing a part in the high temperature laser sintering process. The cooling is so slow that a very high degree of chain re-organisation is possible, especially for the

chain fragments of low molecular weight produced as a result of degradation. Although not constant throughout, during a standard build in the high temperature SLS machine, the PEK powder is cooled at an approximate rate of 0.2°C/min for 36 hours. The effect of higher crystallinity is also reflected in the higher melting temperature of the used HP3 PEK powder in Table 1. A study carried out by Bassett et al., (1988) on crystallisation phenomena on PEEK, noticed a gradual increase in melting temperature with the increase of crystallinity achieved through various cooling and annealing processes.

Material	Crystallinity (%)	Peak T _{m1} (°C)	Peak T _{m2} (°C)	Peak T _{c1} (°C)	Peak T _{c2} (°C)
Virgin PEK	41.6 ± 3.9	323.6 ± 2.0	372.5 ± 0.5	-	332.1 ± 0.2
Used PEK	52.1 ± 3.0	-	396.6 ± 0.9	278.3 ± 3.6	293.61 ± 2.3

Table 1 Crystallinity, melting temperature (T_{m1}, T_{m2}) and crystallisation temperatures (T_{c1}, T_{c2}) for virgin and used HP3 PEK powder

Figure 6 shows standard heating and cooling DSC thermograms of virgin and used PEK powder.

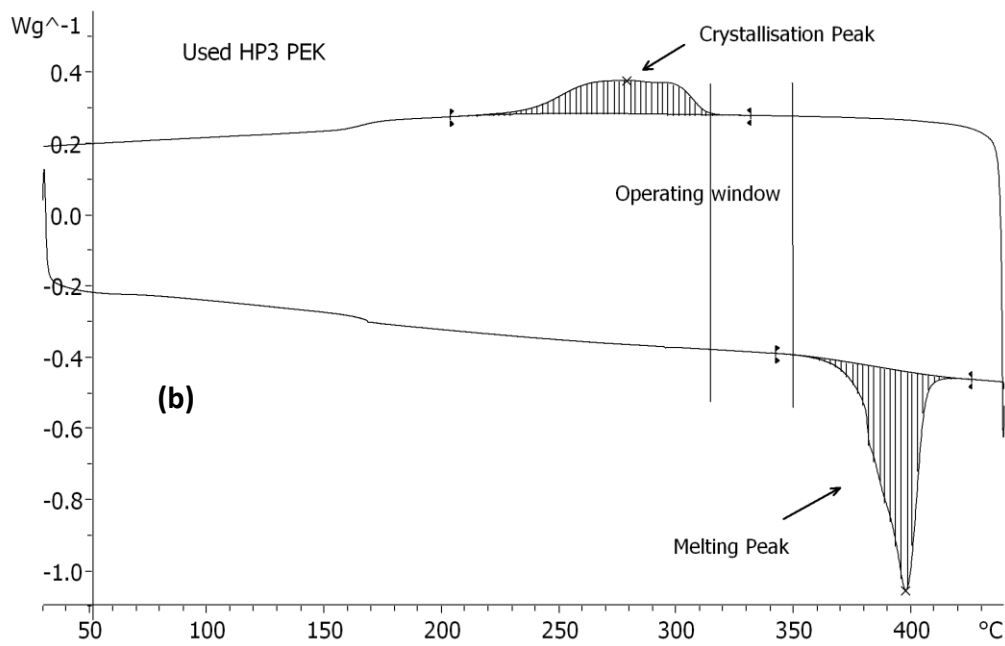
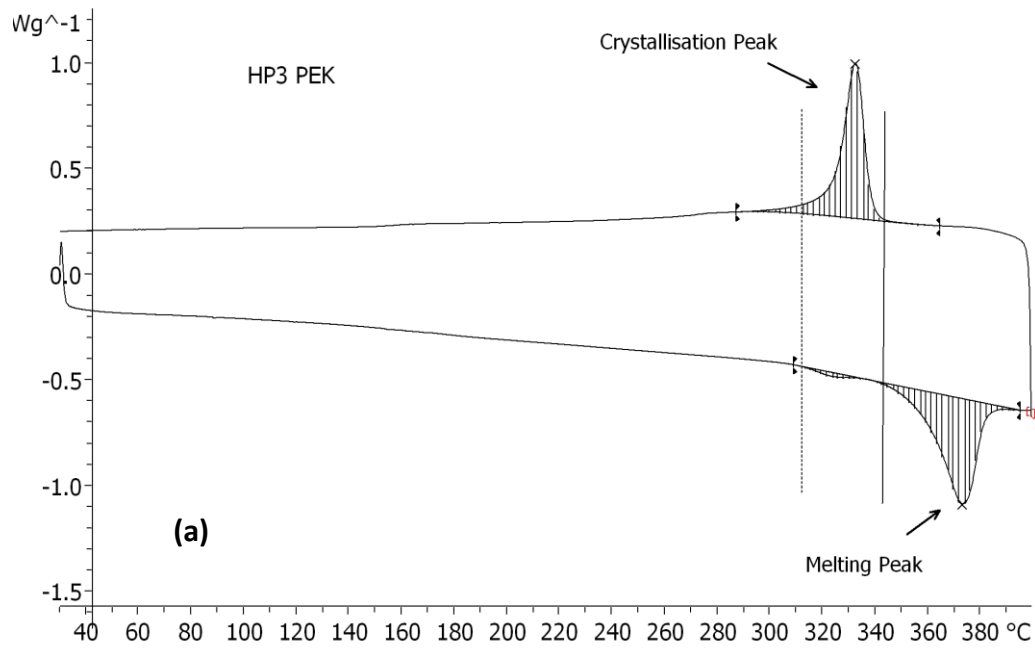


Figure 6 DSC thermogram of (a) virgin and (b) used HP3 PEK powder

It is interesting to note in Table 1 and Figure 6 that the used HP3 PEK powder has a much higher melting temperature in comparison with virgin powder. This is not

surprising as for a higher degree of crystallinity, which is the case of used HP3 PEK powder, the melting temperature is also higher. Gardner et al. (1992) noticed a similar effect. It is possible that the higher melting temperature is the result of higher quality crystals being formed due to the slow cooling. The original double melting peak is the result of the powder manufacturing process. The “tempering” process introduced by Muller et al., (2008), (annealing) applied to the SLS powder leads to the formation of the double peak.

The used PEK powder presented a wide crystallisation region spread over approximately 90°C. In many cases several crystallisation peaks could be inferred, however two peaks were clearly noticeable in all traces and therefore included in Table 1. The presence of multiple crystallisation peaks suggests degradation with reduction of molecular weight. Shorter chain lengths lead to increased chain mobility, higher quality crystals formation and higher degree of crystallinity overall. However, crosslinking is also present as shown by the reduced viscosity measurements; the degradation process of used PEK gives both shorter molecular weight chains and cross-linked structures. Hay and Kemmish (1987) showed that the radicals produced during the random homolytic scission of the ethers, combine intra and intermolecularly to produce cross-linked structures such as benzofuran derivatives presented in Figure 7 (a). Day et al., (1990) suggested the possibility of a different cross-linking product for PEEK which could follow a similar mechanism in PEK. The chemical structure is presented in Figure 7(b). The re-arrangement structure proposed originally by Day et al., (1990), was also accepted by Patel et al., 2010, in their review on mechanism of thermal decomposition of PEEK. Day et al.,

(1990) used ^{13}C Nuclear Magnetic Resonance data to support their theory. However, as stated by Patel et al. (2010), the structure is not entirely verified by their results.

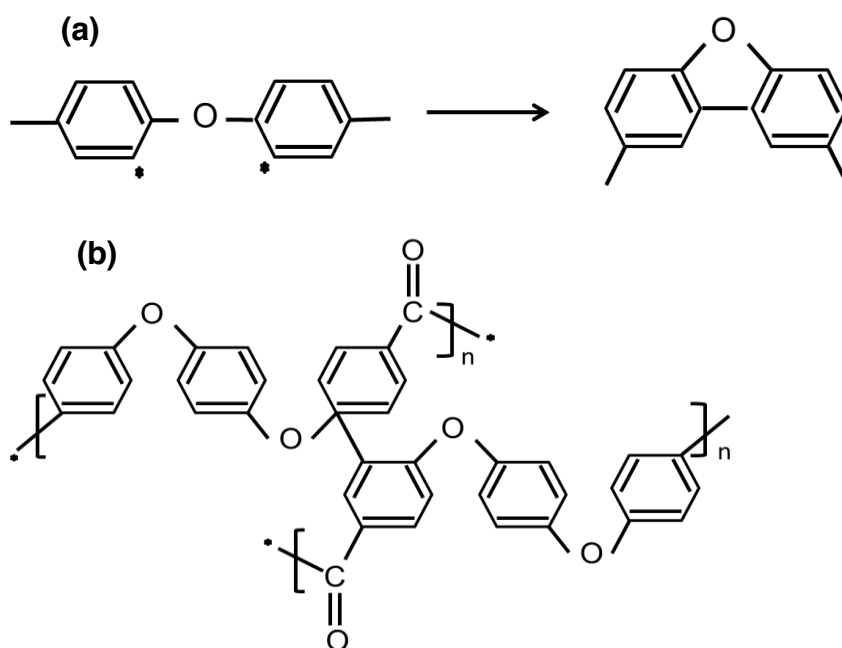


Figure 7 Possible cross-linking structures (a) Internal recombination of PEK and PEEK radicals (Hay and Kemmish, 1987); (b) slow re-arrangement process (Day et al., 1990, Patel et al., 2010)

It is possible that these cross-linked structures are present in this study, however further investigations would be required to confirm their exact structures.

The thermal boundary condition is another interesting aspect of this study. In their study, Kruth et al. (2008) explained that the temperature difference between the melting and crystallisation points/regions (known also as operating or consolidation window) is key to the sintering process such that the cooling profile along this region determines ultimately the final properties of the materials. A slow crystallisation process as well as a large temperature difference between the endothermic (T_m) and exothermic (T_c) peaks normally leads to good quality parts.

The melting and crystallisation regions of virgin PEK powder, in Figure 6, lacks this “consolidation window” and even overlap, whereas the used PEK presents a temperature difference of approximately 50°C. According to Kruth et al. (2008), polymers missing this consolidation window do not sinter well. However, this was not the case in our study where virgin PEK powder sintered well following the process described in Section 2.2. It is not clear whether this behaviour pertains only to laser sintering of high temperature polymers, but based on this theory, the large processing window recorded in the used powder makes used HP3 powder a better polymer candidate for further use in SLS than virgin PEK.

4.4 Tensile Testing

Tensile strength and elongation at break of the HP3 PEK powder and the two blends of used and virgin PEK powders are presented in Figure 8 and Figure 9.

A decrease of up to 17% in tensile strength and 16% in elongation at break was noticed with incorporation of 30% used PEK. In contrast, Zarringhalam et al. (2006) showed for additive manufactured nylon parts, a significant increase in elongation at break when a higher percentage of reuse powder was incorporated during SLS. The authors suggested that the higher molecular weight is responsible for the higher ductility noticed in used nylon. In comparison with nylon, the increased molecular weight observed during PEK degradation is the result of cross-linking and branching rather than single long chain formation (Hay and Kemmish, 1987). The degradation mechanism of PEEK and PEK proposed by Hay and Kemmlish (1987) was random homolytic scission; with formation of a large number of molecular ions and fragmentation sequences as well as cross-linked, bulky structures (through

recombination of radicals); identified using mass spectroscopy and GPC gel permeation chromatography. The higher crystallinity values of used PEK coupled with the slight decrease in elongation at break of samples incorporating used powder are in agreement with the PEEK results of Chivers and Moore (1994), who noticed a decrease in ductility with increase of crystallinity.

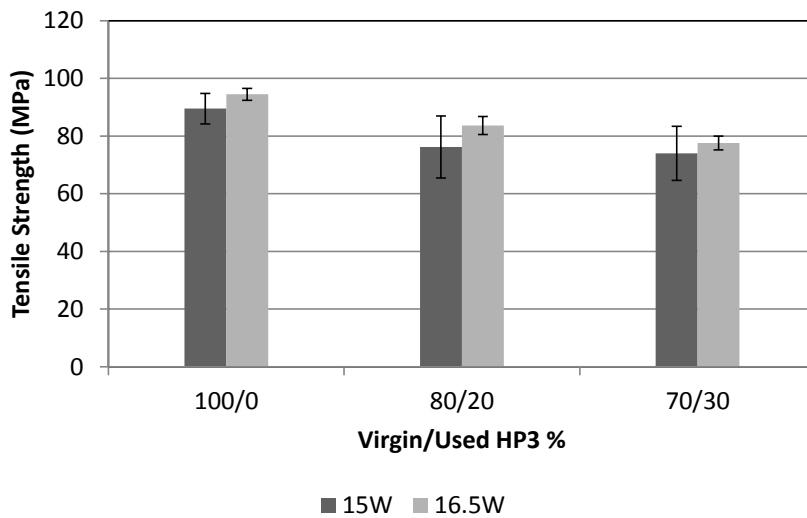


Figure 8 Tensile strength for virgin/used HP3 PEK blends sintered at 15W and 16.5W laser power

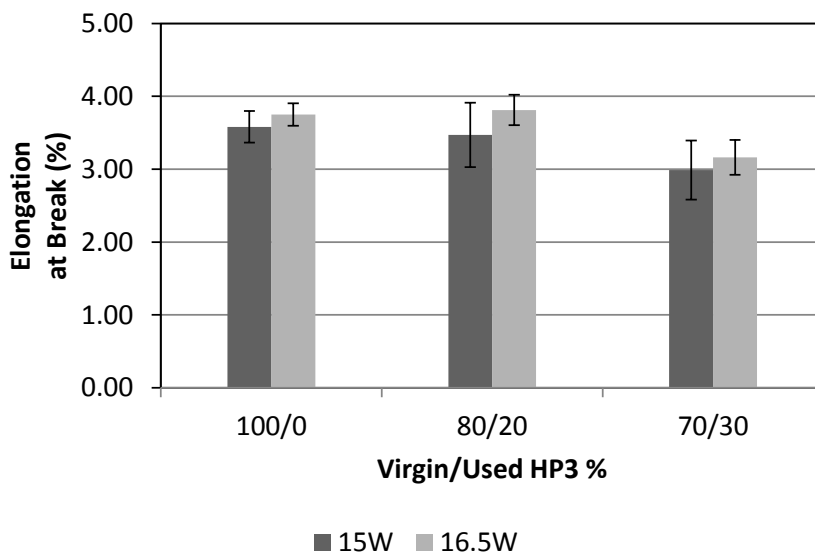


Figure 9 Elongation at Break for virgin/used HP3 PEK blends sintered at 15W and 16.5W laser power

It is interesting to notice that in spite of the confirmed degradation of the used PEK particles, the strength and the elongation of the parts incorporating used PEK material are still relatively high. It is possible that the appearance of an operating window (see Figure 6) in used HP3 PEK powder particles makes the sintering of the two blends possible, allowing enough time for re-ordering and re-crystallisation of the unaltered or shorten chains along the bonded, necking region of two particles. Figure 10 illustrates two proposed re-ordering scenarios within virgin and used particles when (a) the re-ordering takes places across the entire necking region or (b) there is only a partial chain re-ordering and bonding taking place due to the presence of cross-linked sites. When the re-ordering and re-crystallisation between used and virgin is possible (Scenario (a) in Figure 10), the crystalline phases of the two particles are merging and therefore a good neck growth is achieved which is an indication of a good sintering process. However, the presence of cross-linked sites can interfere with the neck growth of the used and virgin particles (see Scenario (b) in Figure 10), in which case there will be only a partial merging in crystallisation sites and ultimately a poor bonding which leads to high porosity and low mechanical strength.

The hot stage sintering images of virgin and used particles in Figure 11, Figure 12 and Figure 13 confirm the re-ordering and sintering theory proposed in Figure 10. As it can be seen in Figure 11, the used particles do not fully melt/bond, retaining the neck shape even at 440°C.

The sintering of two virgin particles, in Figure 12, shows a completely different behaviour, the particles coalesce fully at 440°C and form one large molten particle, losing completely the neck area.

The difference in coalescence behaviour of a virgin and used particle is visually very clear. All images in Figure 13 show that the used particle is barely changing shape, not melting, where the virgin particle is melting, it connects to the used particle wanting to coalesce to the particle close in its vicinity. Once again, the virgin particle is fully melted at 440°C, where the used one is not showing any signs of melting.

Based on the images shown in Figure 11 to Figure 13 it is also clear that the rate of coalescence is very different.

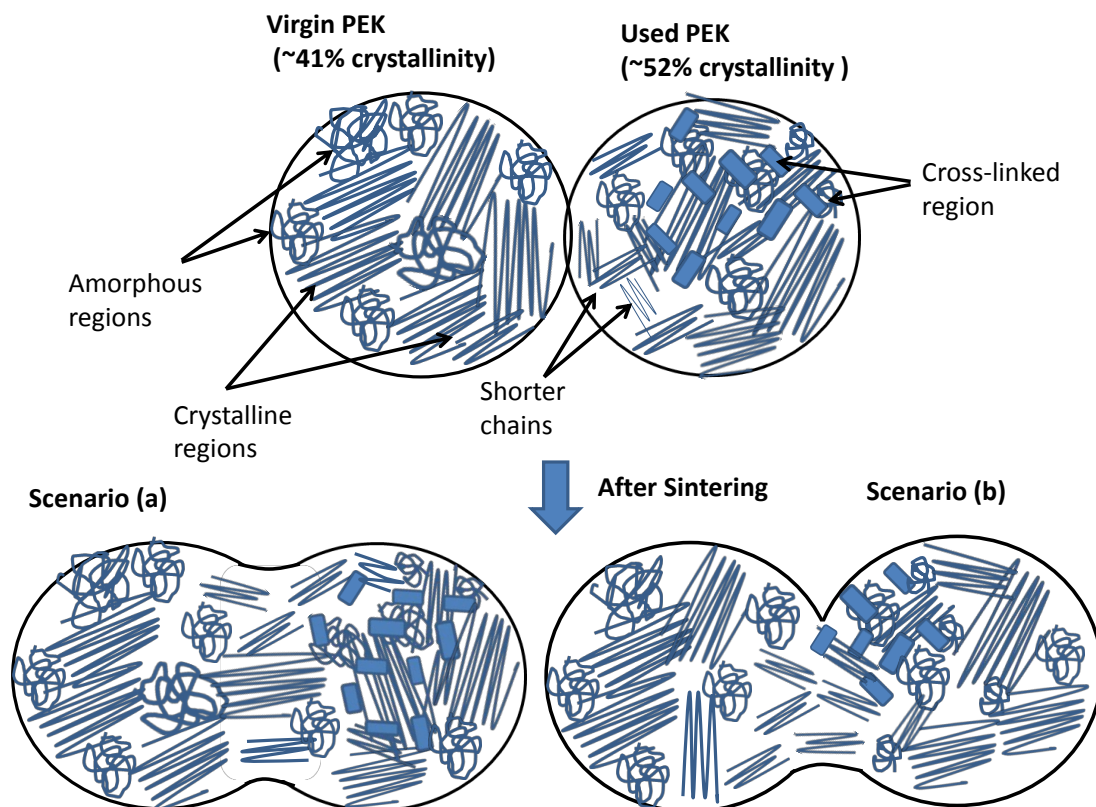


Figure 10 Re-ordering options of molecular chains during sintering



Figure 11 Used particles at 374, 400, 440°C



Figure 12 Virgin particles at 381, 391 and 440°C

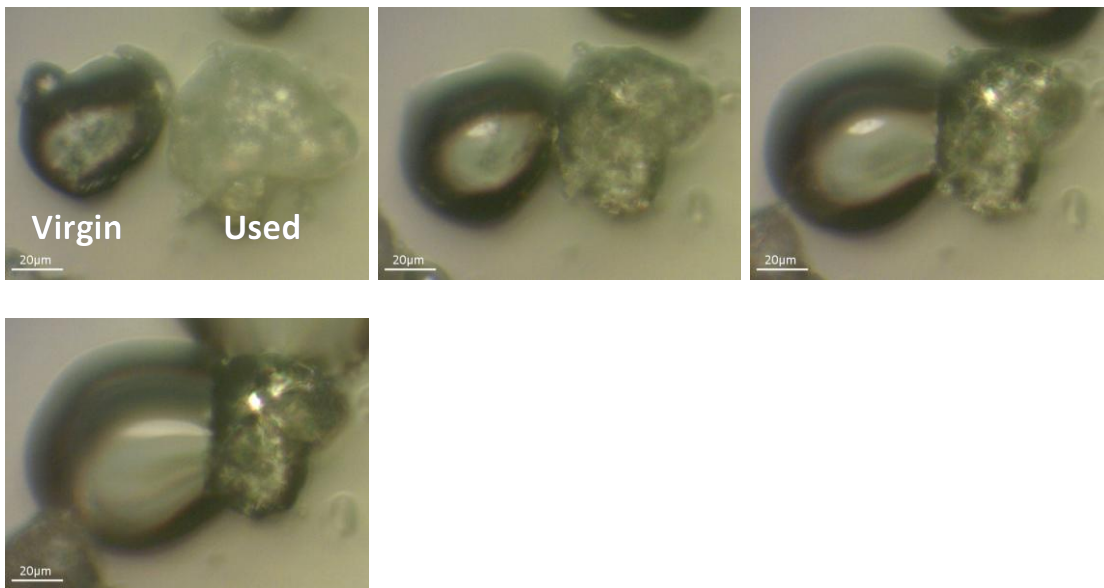


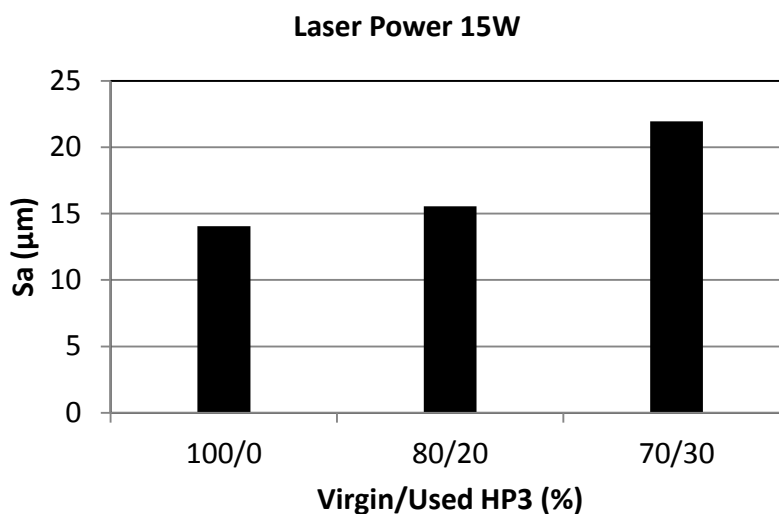
Figure 13 Virgin and used particles at 385, 403, 413, 440° C

4.5 Surface Topology Measurements

Figure 14 presents the XY surface roughness of parts produced using virgin and virgin/used HP3 PEK blends. At standard laser power (15W), the effect of adding used HP3 PEK powder is easily observed through an increase in surface roughness. This was attributed to the slightly higher particle size distribution encountered in the used HP3 powder in comparison with virgin HP3 material (see Figure 5) and the difference in melting temperature between used and virgin HP3 PEK powder (see Table 1). The standard laser power, 15W, is not sufficient for good sintering of the used HP3 material which presents an approximately 20°C increase in melting temperature.

Higher laser power (16.5W) reduced the differences in surface roughness between the parts made using virgin HP3 PEK powder and those using blends of virgin and used HP3 powder. Higher laser power inputs more energy into the laser sintering process and leads to increased connectivity between particles and better bonding. Higher energy results also in higher heating temperatures closer to the melting temperature of the used HP3 PEK powder, which leads to a better surface quality.

(a)



(b)

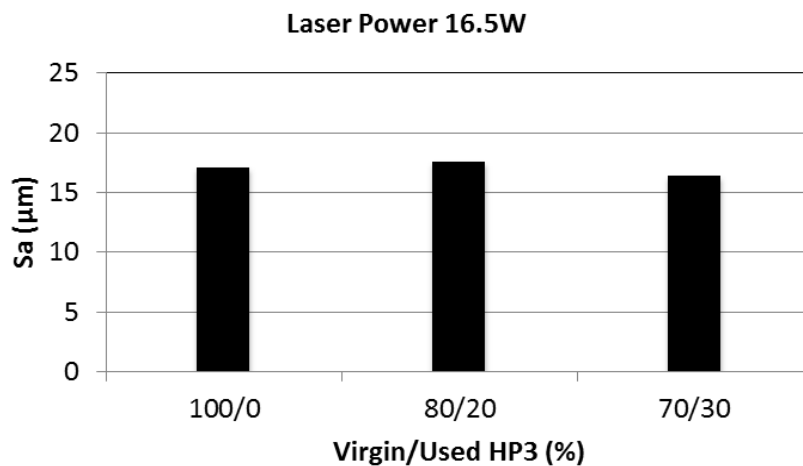


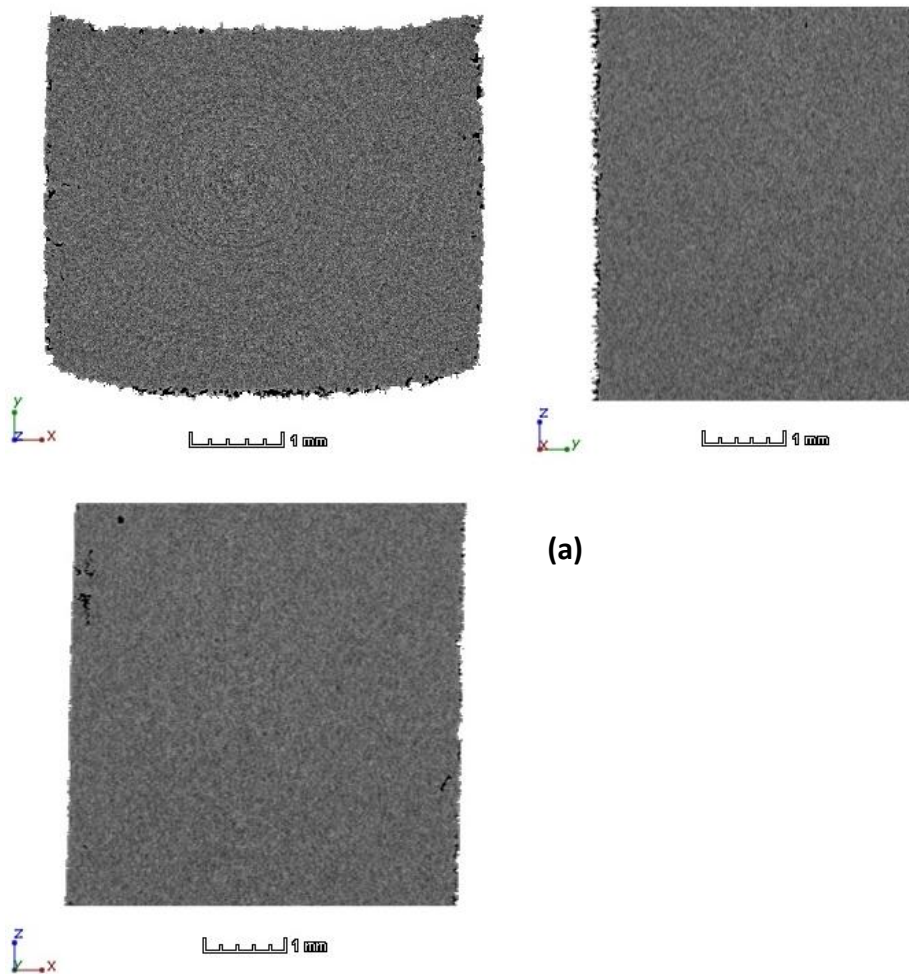
Figure 14 Surface roughness of SLS HP3 parts build using 100/0; 80/20 and 70/30 % virgin/used powder blends at (a) 15W laser power and (b) 16.5W laser power.

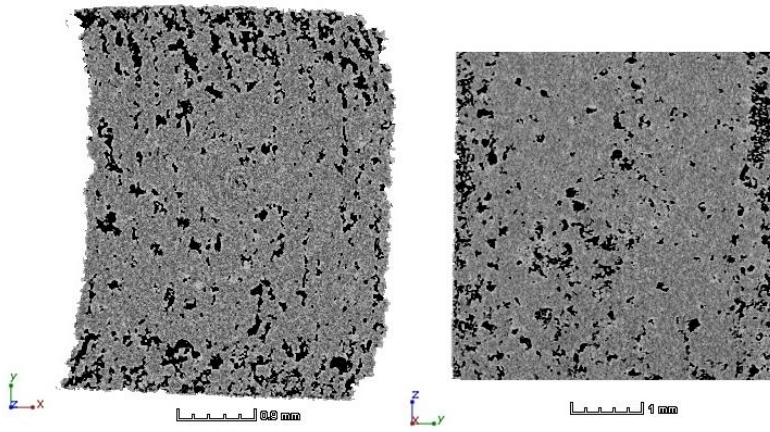
Surface roughness is an important parameter in the manufactured parts, which is also related to mechanical performance, therefore has received significant importance in the past. For example, Beard et al., 2011, showed that there is a clear correlation between the laser scan speed or scan power and the surface roughness due to the degree of sintering between particles (particle neck growth). Dotchev and Yusoff (2009) carried out an extensive study on the relationship between the melt flow index (MFI) and “orange peel” effect and concluded that in order to avoid orange peel texture, a minimum recommended value of 25-26g/10min(MFI) should

be used for nylon powder (virgin or refreshed). Although MFI gives good comparative indication of viscosity behaviour which can be related to degradation effects, changes in the particle size distribution should be also considered as they would affect the “orange peel” behaviour.

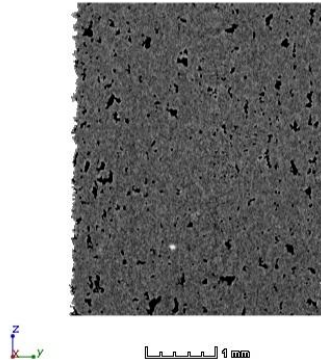
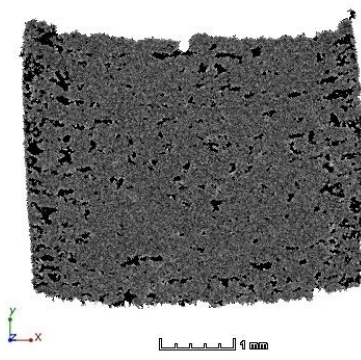
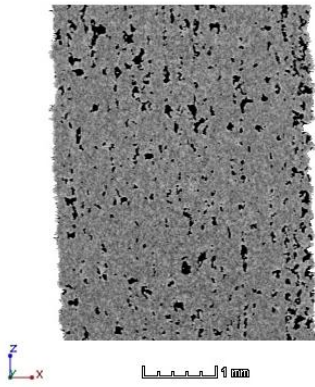
4.6 Micro Computer Tomography (μ CT)

Micro-CT images of small cubes cut out of the tensile test specimens of virgin HP3 and 80/20, 70/30% virgin/used HP3 PEK blends are presented in Figure 15 and Figure 16, respectively.





(b)



(c)

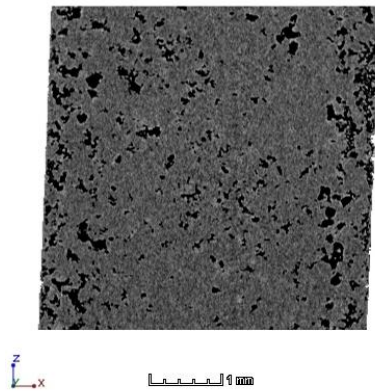


Figure 15 Micro-CT scans of (a) 100% PEK HP3; (b) 80/20% virgin/used PEK; (c) 70/30% virgin/used PEK (All samples sintered at 15W)

Figure 15 clearly shows that the introduction of the used PEK powder led to high porosity in the sintered part: 99.7 % global density for 100 % virgin PEK; 89.6 % global density for 80/20 % virgin/used PEK and 93.4 % for 70/30 % virgin/used PEK.

These results confirm and help explain the mechanical test results; higher porosity means a weaker structure and increased flaws for cracks propagation.

However, the use of higher power can help reduce significantly the porosity. For example, Figure 15 shows that a 10% increase in laser power for 80/20 % virgin/used PEK leads to approximately 9% increase in global density (98.9 % at 16.5W).

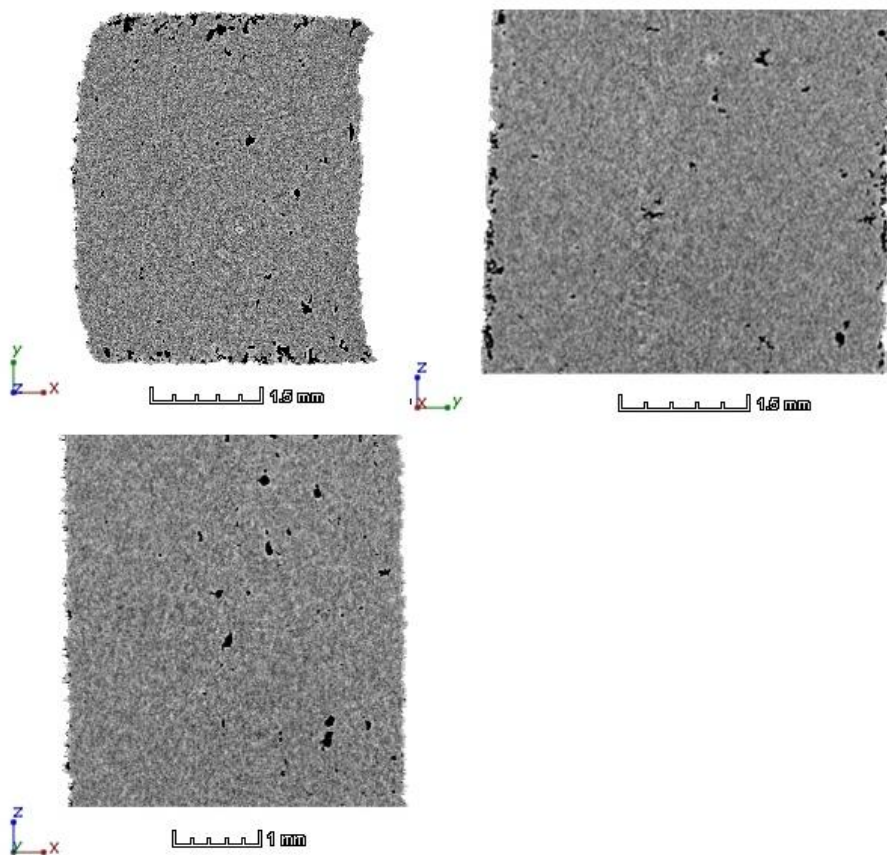


Figure 16 Micro-CT scans of 80/20 % virgin/used PEK at 16.5W laser power.

This proves that process optimisation is important even when reusing the same materials. The proposed sintering mechanism of virgin and used PEK particles, in Figure 10, is confirmed by the micro-CT results. When cross-linking sites are present in the necking region, the sintering cannot take place within the allocated process time and therefore a reduced necking region is formed which is reflected in higher porosity.

Conclusions

This paper gives, for the first time, insights into the physico-chemical behaviour of virgin and used PEK powders and parts in high temperature selective laser sintering using bespoke high temperature selective laser sintering equipment (EOS P800). Although the used PEK powder incurs degradation, the reuse of PEK powder in laser sintering of new parts is possible with little effect on mechanical performance. A sintering mechanism of virgin and used PEK particles is proposed and confirmed by the hot stage images of various PEK particles coalescing. The 10% increase in laser power has no significant effect on the tensile properties or the intrinsic microstructure of the parts (investigated through micro-CT) but improved the surface finish of the manufactured parts.

Acknowledgements

The authors would like to thank Mr Pierluigi Quarato for support with the surface analysis measurements and Dr Andy McLaughlin for technical discussions. The technical support of the entire CALM team is also acknowledged.

References

Bassett D.C., Olley R.H., Al Raheil I. A. M., (1988) On crystallization phenomena in PEEK, *Polymer*, 29, 1745-1754

Beard, M. A., Ghita, O. R., Bradbury, J., Flint, S., and Evans, K. E. (2011) Material Characterisation of Additive Manufacturing Components Made From a Polyetherketone (PEK) High Temperature Thermoplastic Polymer, In *Advanced Research in Virtual and Rapid Prototyping (VRAP)* (Bartolo, P. J., Ed.), Leiria, Portugal.

Blundell, D. J., & Osborn, B. N., 1983, The morphology of poly(aryl-ether-ether-ketone). *Polymer*, 24(8), 953–958

Cebe P., 1988, Annealing study of poly(etheretherketone), *Journal of Polymer Science*, Vol. 23, 3721

Chivers, R. A., & Moore, D. R., 1994, The effect of molecular weight and crystallinity on the mechanical properties of injection moulded poly(aryl-ether-ether-ketone) resin. *Polymer*, 35(1), 110–116

Day M., Sally D., Wiles D.M., 1990, Thermal degradation of Poly (aryl-Ether-Ether Ketone): Experimental Evaluation of the Crosslinking Reaction, *Journal of Applied Polymer Science*, 40, pp. 1615-1625

Dotchev, K., and Yusoff, W., 2009, Recycling of polyamide 12 based powders in the laser sintering process, *Rapid Prototyping Journal* 15, 192-203

EOS, 2010, P800 Manual, Application notes on EOS PEEK HP3 for EOSINT P800

EOS, 2013, http://www.eos.info/systems_solutions/plastic/systems_equipment

Gardner, 1992, Gardner K.H., Hsiao B.S., Matheson R.R., Wood N. B.A., (1992) Structure, crystallization and morphology of poly (aryl ether ketone ketone), POLYMER, Vol. 33, no. 12, pp. 2483

Gornet, T. J., Davis, K. R., Starr, T. L., and Mulloy, K. M. (2002) Characterization of Selective Laser Sintering Materials to Determine Process Stability, In Proceedings from the Solid Freeform Fabrication Symposium (al, D. B. e., Ed.), pp 546-553, University of Texas at Austin.

Hay, J. N., & Kemmish, D. J., 1987, Thermal decomposition of poly(aryl ether ketones). *Polymer*, 28(12), 2047–2051

Kruth, J. P., Levy, G., Schindel, R., Craeghs, T., and Yasa, E., 2008, Consolidation of Polymer Powders by Selective Laser Sintering, In 3rd International Conference PMI2008, Ghent, Belgium

Kumar, S and Kruth, J-P, 2010, Composites by rapid prototyping technology, *Materials and Design*, Vol. 31(2), 850-856

Martínez A., Ibáñez A., Sánchez A., León M.A., 2011, Comparison of aged polyamide powders for selective laser sintering, *AIP Conf. Proc.* 1431, 5-13

McLauchlin A., Ghita O., Savage L., 2014, Studies on the Reprocessability of Poly(Ether Ether Ketone) (PEEK), *Journal of Materials Processing Technology*, 214, pp. 75-80

Muller F., Pfister A., Leuterer M., 2008, Patent no US 7,847,057 B2, PAEK powder, in particular for the use in a method for a layer-wise manufacturing of a three-dimensional object, as well as method for producing it

Patel P., Hull T. R., McCabe R.W., Flath D., Grasmeder J., Percy M., (2010) Mechanisms of Thermal Decomposition of Poly(Ether Ether Ketone) (PEEK) from a Review of Decomposition Studies, *Polymer Degradation and Stability*, 95, pp. 709-718

Pohle, D., Ponader, S., Rechtenwald, T., Schmidt, M., Schlegel K.A., Münstedt, H., Neukam, F.W., Nkenke, E. & von Wilmsowky, C., 2007, Processing of three-dimensional laser sintered polyetheretherketone composites and testing of osteoblast proliferation in vitro, *Macromolecular Symposia* 253(1):65-70.

Rechtenwald, T., Esser, G., Schmidt, M., and Pohle, D., 2005, Comparison between Laser Sintering of PEEK and PA using design of experiment methods, In *Advanced Research in Virtual and Rapid Prototyping (VRAP)* (Bartolo, P. J., Ed.), 343-348, Leiria, Portugal.

Schmidt, M., Pohle, D., and Rechtenwald, T., 2007, Selective laser sintering of PEEK, *Cirp Annals-Manufacturing Technology* 56, 205-208

Shi, Y., Li, Z., Sun, H., Huang, S., and Zeng, F. (2004) Effect of the properties of the polymer materials on the quality of selective laser sintering parts, *Proc. Inst. Mech. Eng. Pt. L-J. Mater.-Design Appl.* 218, 247-252

Stout K.J., Sullivan P. J., Dong W.P., Mainsah E., Lou N., Mathia T., Zahouani H., 1993, The Development of Methods for The Characterisation of Roughness in Three Dimensions, Report EUR 15178 EN, EC Brussels

Tan, K.H., Chua, C.K., Leong, K.F., Cheah, C.M., Cheang, P., Abu Bakar, M.S. & Cha, S.W., 2003, Scaffold development using selective laser sintering of poly ether ether ketone hydroxyapatite biocomposite blends. *Biomaterials* 24(18): 3115-3123.

Victrex, 2013, <http://www.victrex.com/en/victrex-library/datasheets/datasheets.php>

Zarringhalam, H., Hopkinson, N., Kamperman, N. F., and de Vlieger, J. J., 2006, Effects of processing on microstructure and properties of SLS Nylon 12, *Mater. Sci. Eng. A-Struct. Mater. Prop. Microstruct. Process.* 435, 172-180

List of Captions

Figure 1 Chemical structure of PEK and PEEK

Figure 2 Reduced build diagram

Figure 3 Diagram of the build

Figure 4 XY area used for surface roughness measurements

Figure 5 Particle size distribution of virgin and used HP3 PEK powder

Figure 6 DSC thermogram of (a) virgin and (b) used HP3 PEK powder

Figure 7 Possible cross-linking structures (a) Internal recombination of PEK and PEEK radicals (Hay and Kemmish, 1987); (b) slow re-arrangement process (Day et al., 1990, Patel et al., 2010)

Figure 8 Tensile strength for virgin/used HP3 PEK blends sintered at 15W and 16.5W laser power

Figure 9 Elongation at Break for virgin/used HP3 PEK blends sintered at 15W and 16.5W laser power

Figure 10 Re-ordering options of molecular chains during sintering

Figure 11 Used particles at 374, 400, 440°C

Figure 12 Virgin particles at 381, 391 and 440°C

Figure 13 Virgin and used particles at 385, 403, 413, 440° C

Figure 14 Surface roughness of SLS HP3 parts build using 100/0; 80/20 and 70/30 % virgin/used powder blends at (a) 15W laser power and (b) 16.5W laser power

Figure 15 Micro-CT scans of (a) 100% PEK HP3; (b) 80/20% virgin/used PEK; (c) 70/30% virgin/used PEK (All samples sintered at 15W)

Figure 16 Micro-CT scans of 80/20 % virgin/used PEK at 16.5W laser power

Material	Crystallinity (%)	Peak T _{m1} (°C)	Peak T _{m2} (°C)	Peak T _{c1} (°C)	Peak T _{c2} (°C)
Virgin PEK	41.6 ± 3.9	323.6 ± 2.0	372.5 ± 0.5	-	332.1 ± 0.2
Used PEK	52.1 ± 3.0	-	396.6 ± 0.9	278.3 ± 3.6	293.61 ± 2.3

Table 1 Crystallinity, melting temperature (T_{m1}, T_{m2}) and crystallisation temperatures (T_{c1}, T_{c2}) for virgin and used HP3 PEK powder

Figure 1
[Click here to download high resolution image](#)

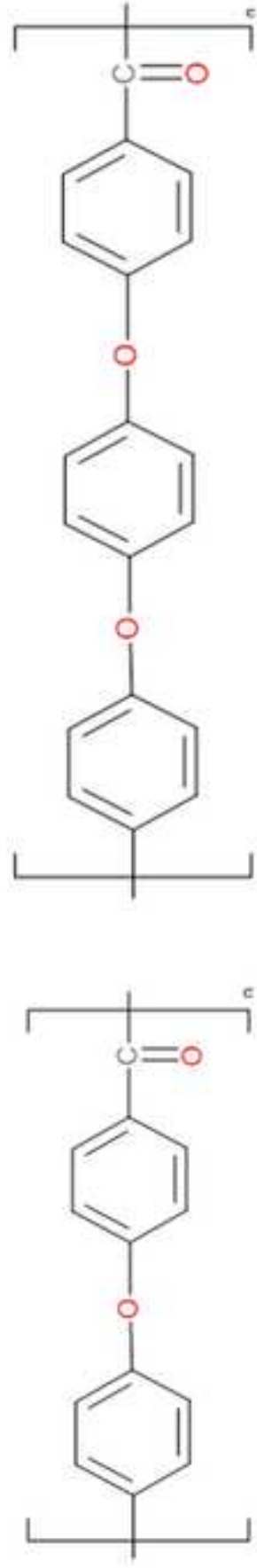


Figure 2
[Click here to download high resolution image](#)

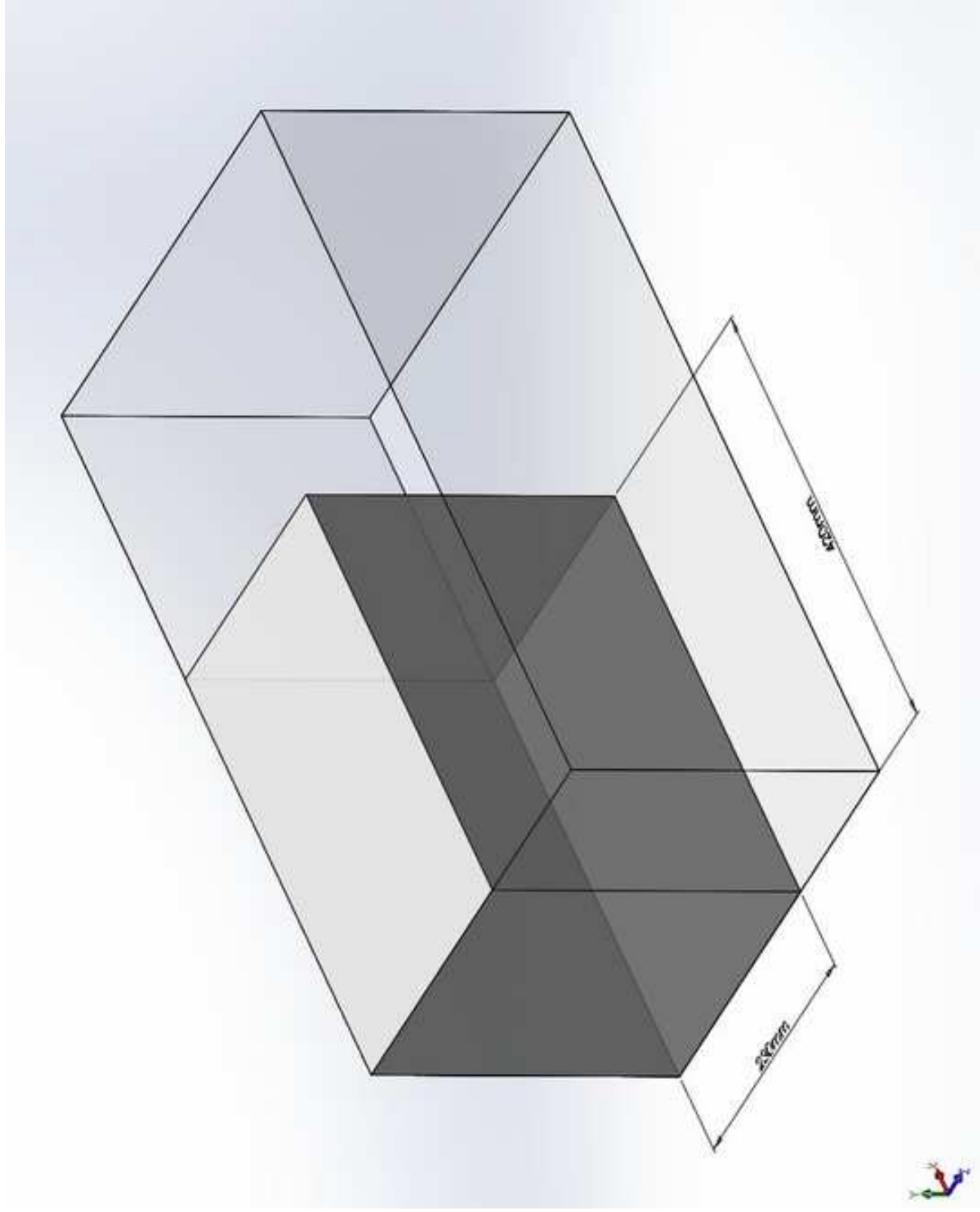


Figure 3
[Click here to download high resolution image](#)

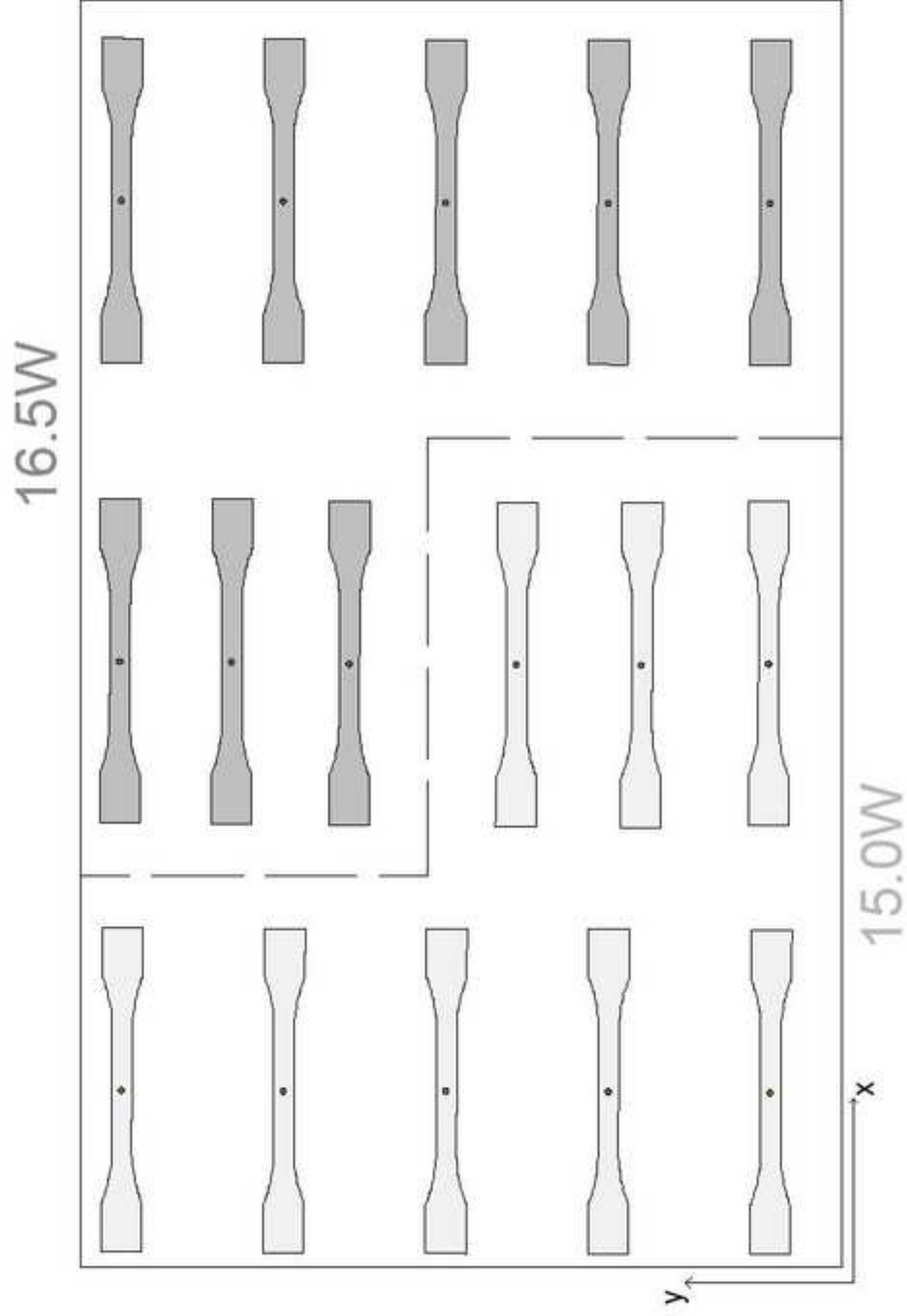


Figure 4
[Click here to download high resolution image](#)

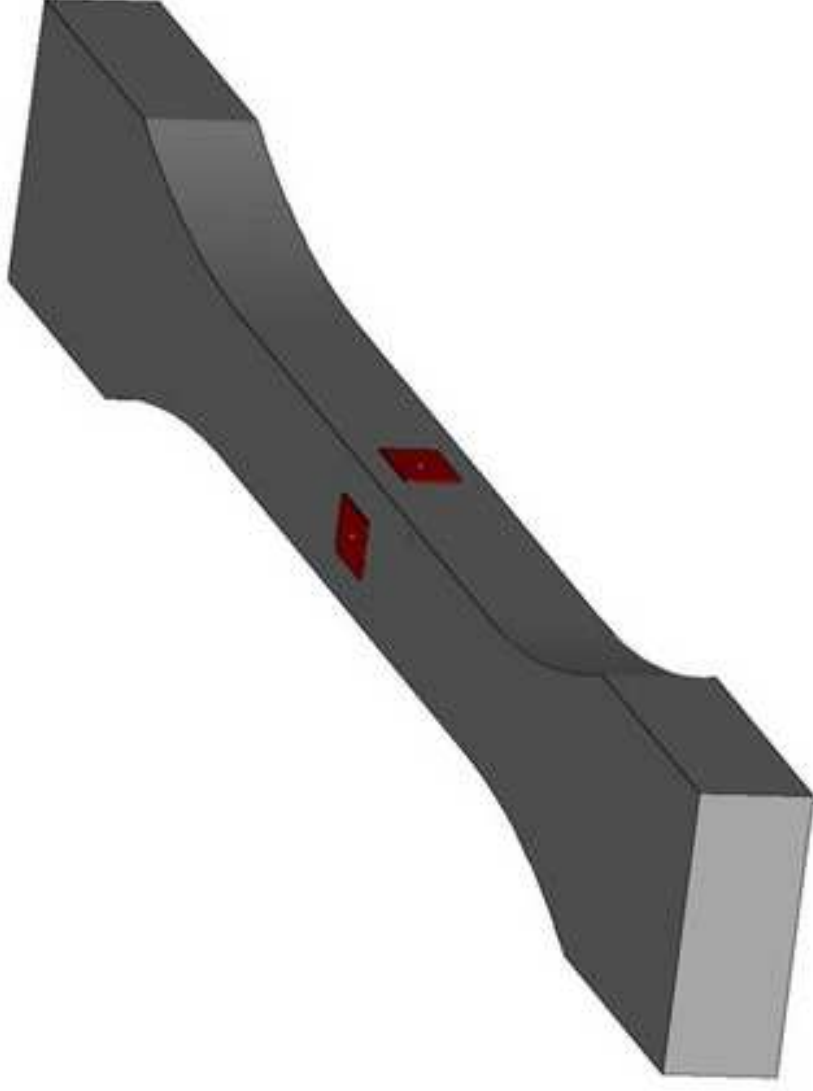


Figure 5
[Click here to download high resolution image](#)

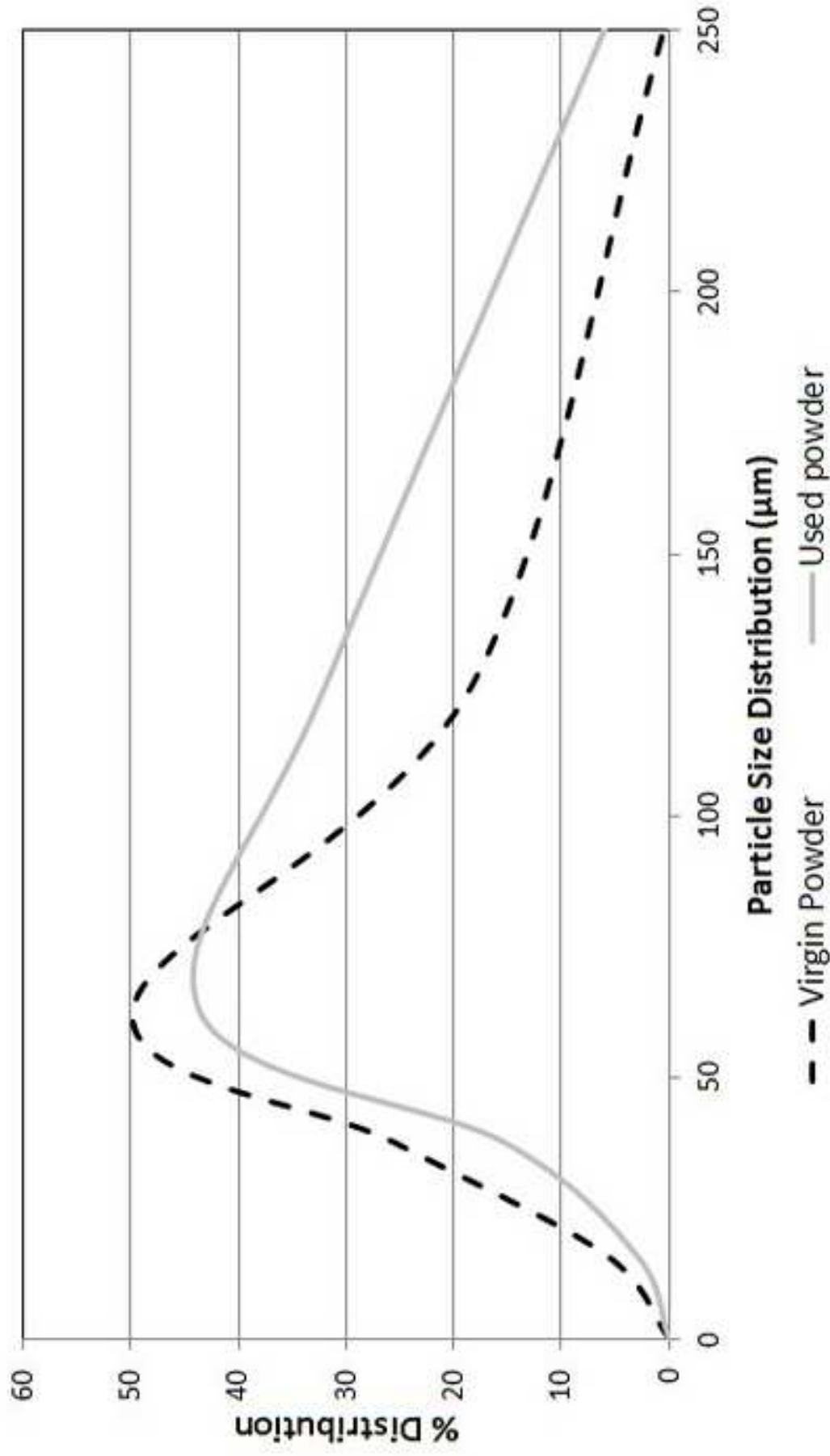


Figure 6a
[Click here to download high resolution image](#)

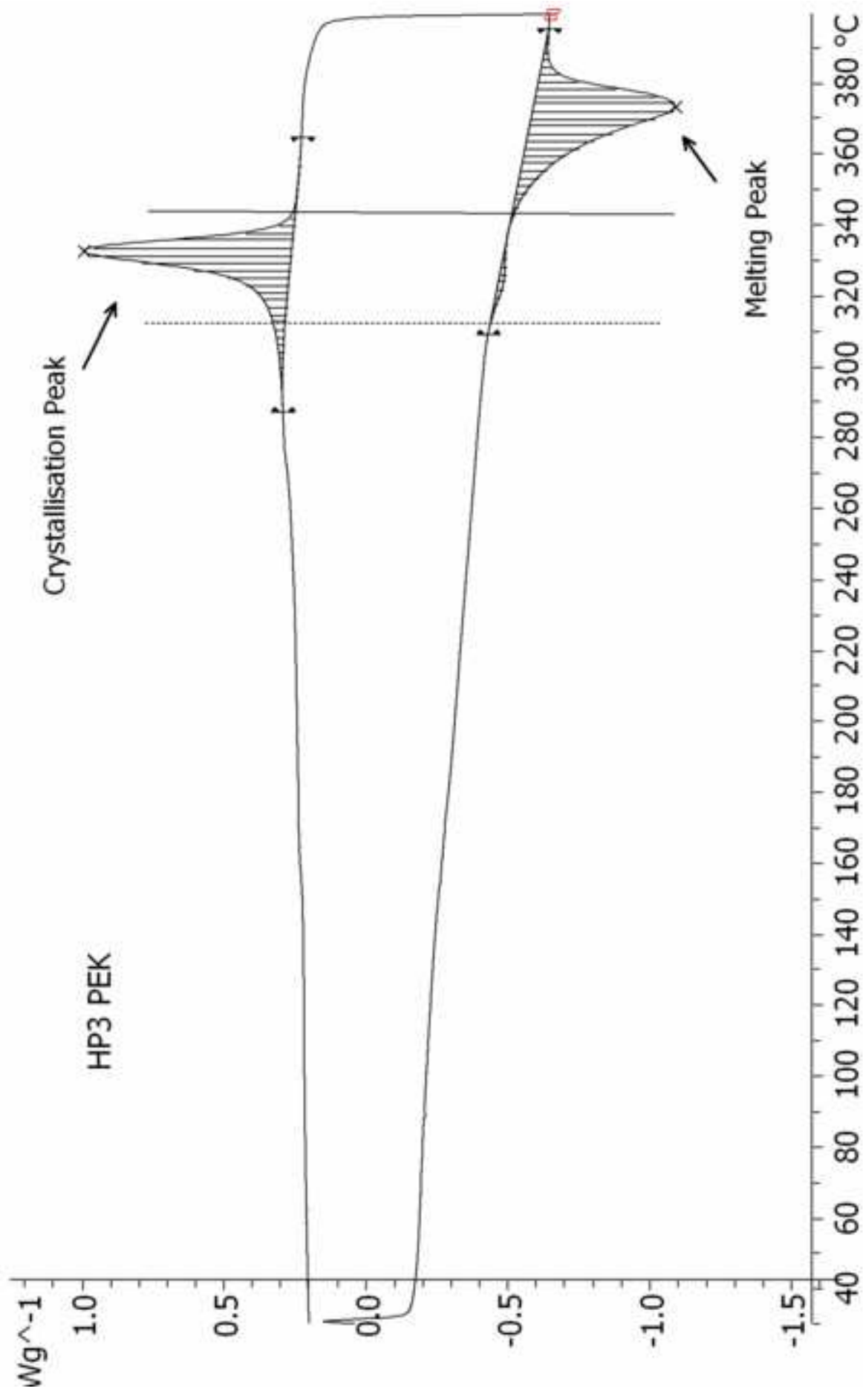


Figure 6b
[Click here to download high resolution image](#)

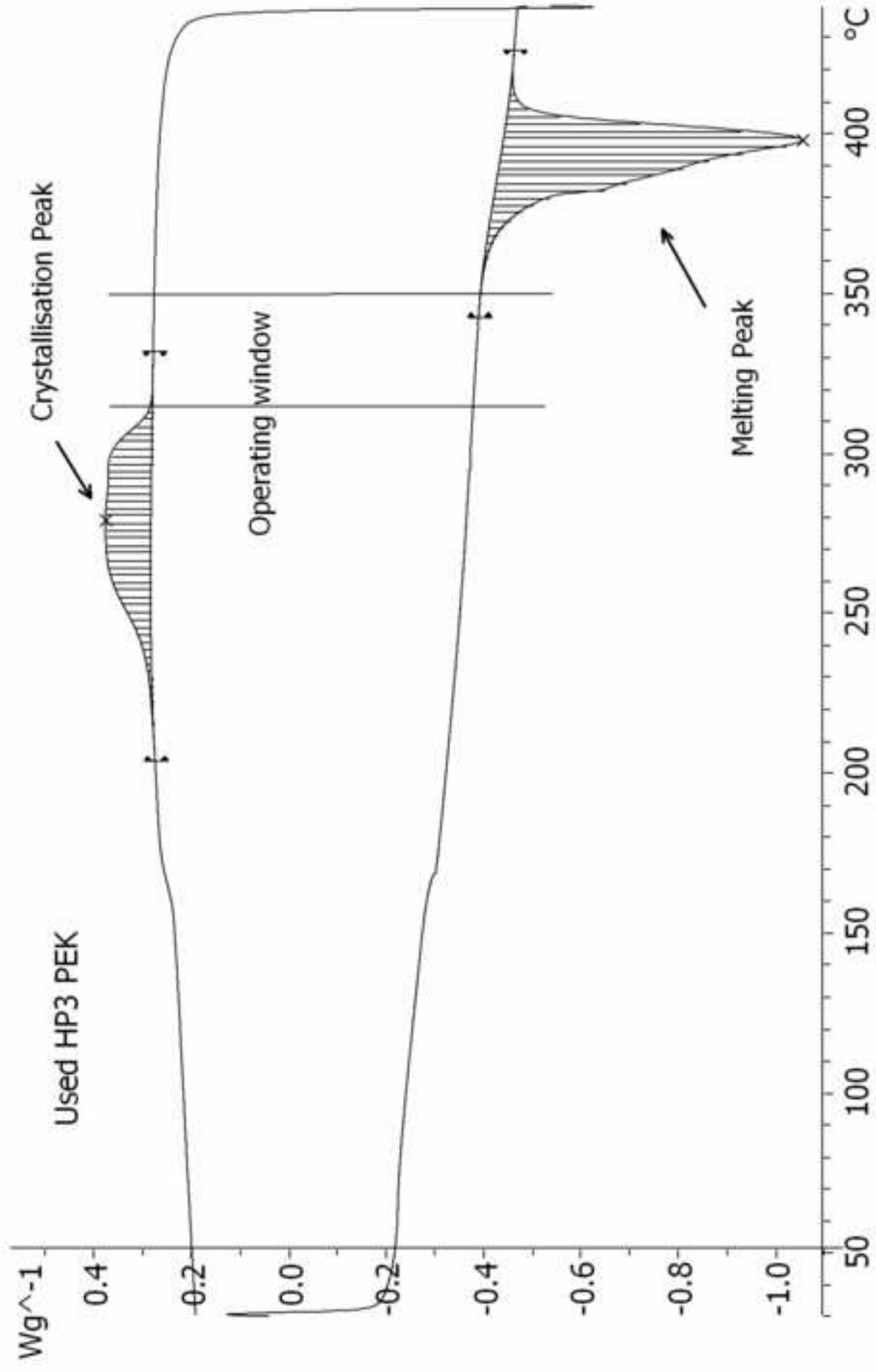


Figure 7a
[Click here to download high resolution image](#)

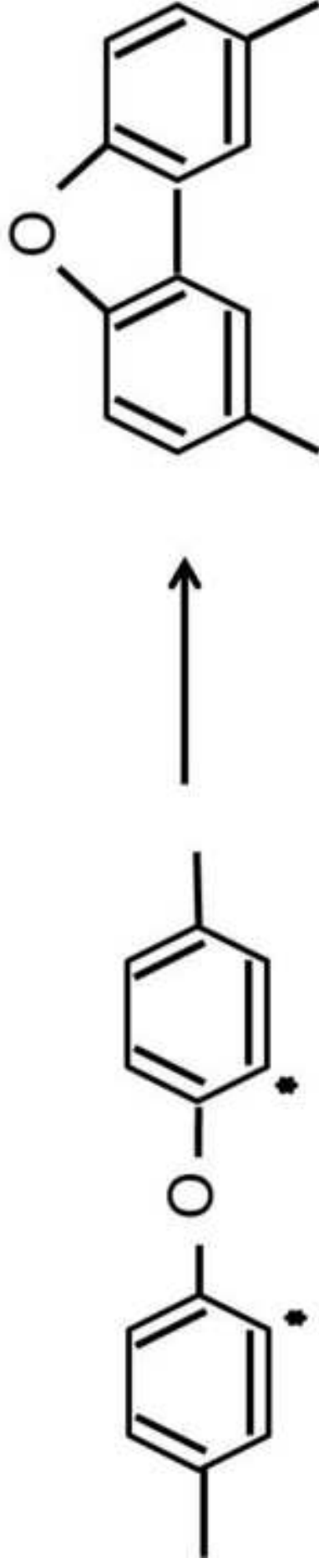


Figure 7b
[Click here to download high resolution image](#)

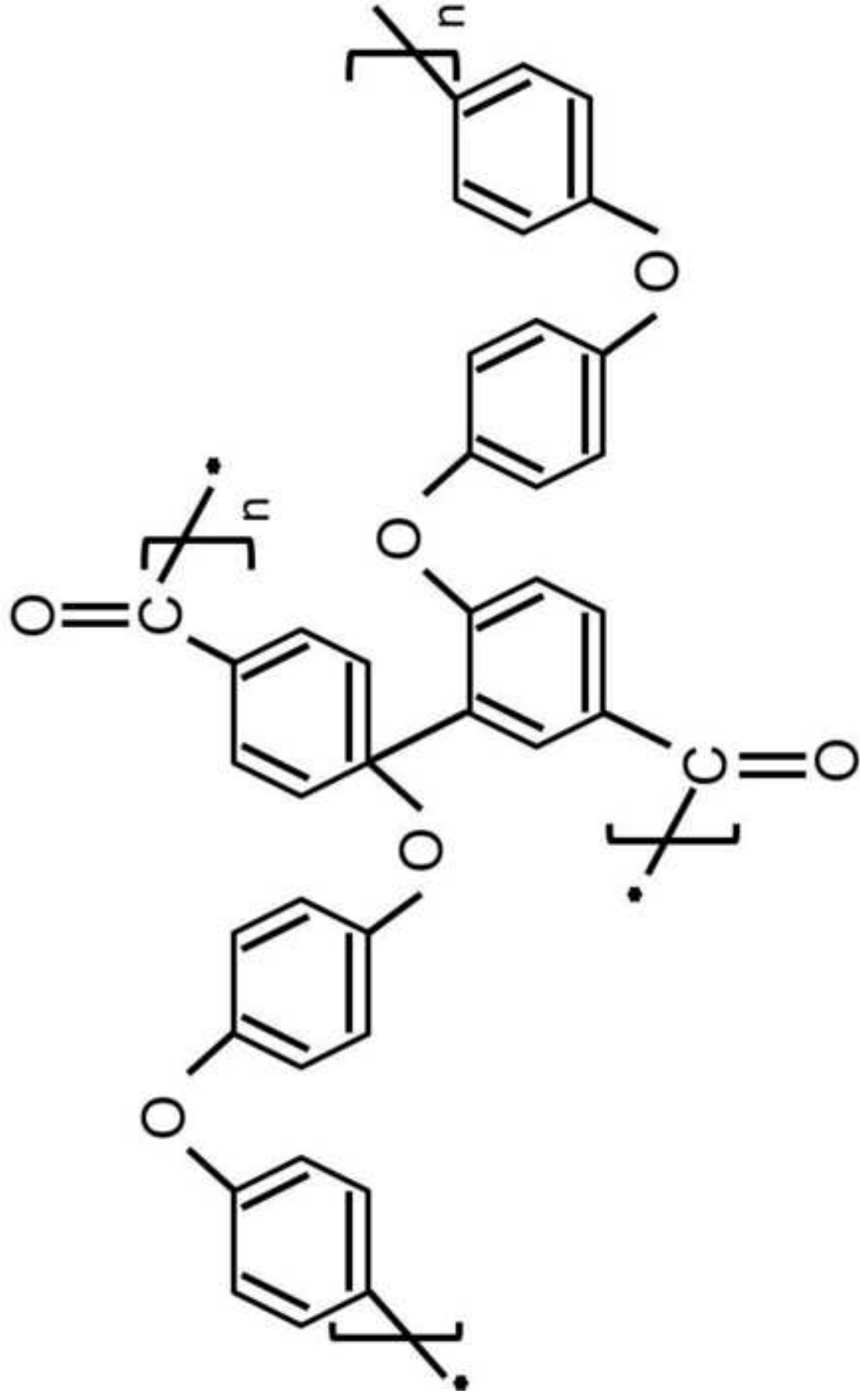


Figure 8
[Click here to download high resolution image](#)

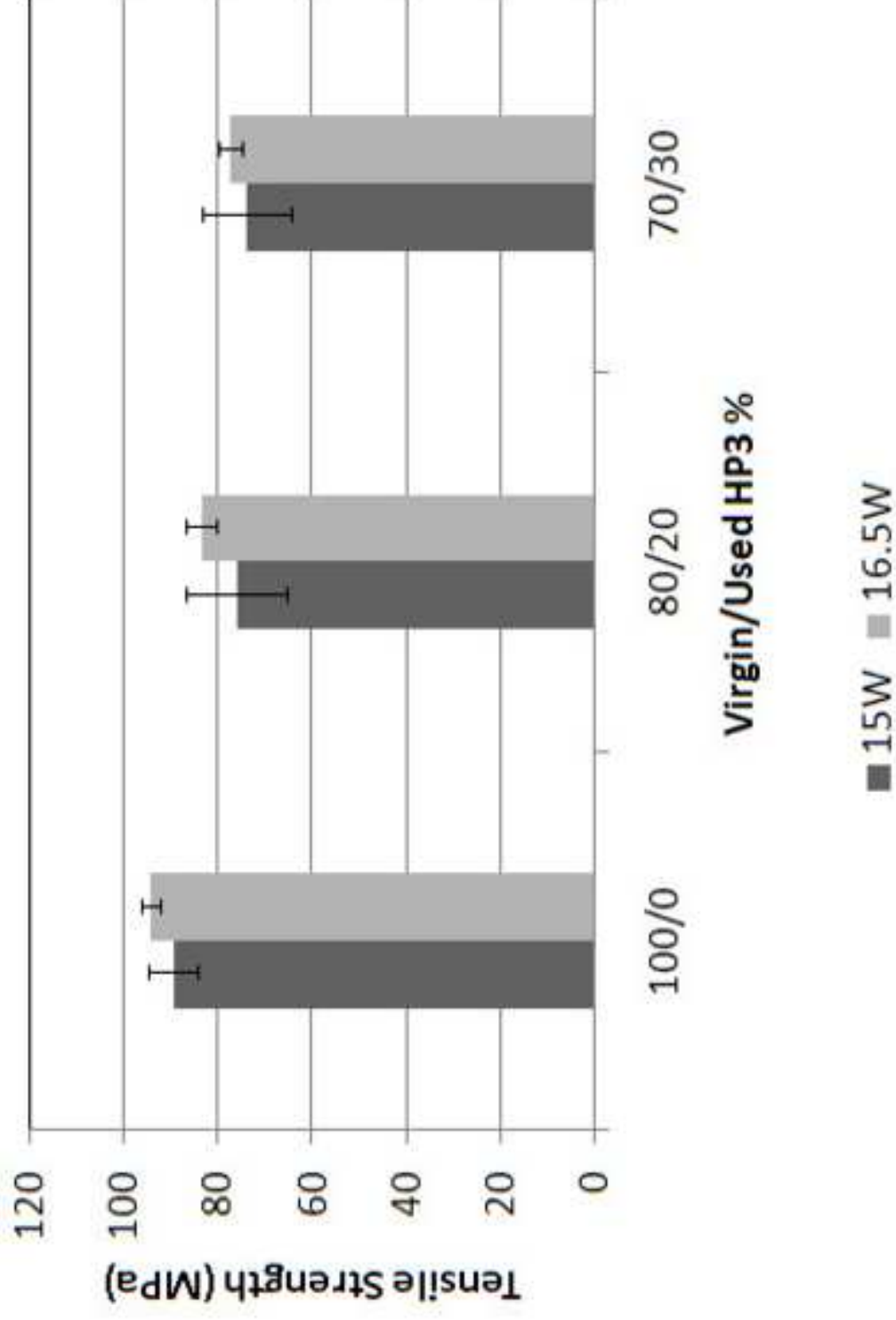


Figure 9
[Click here to download high resolution image](#)

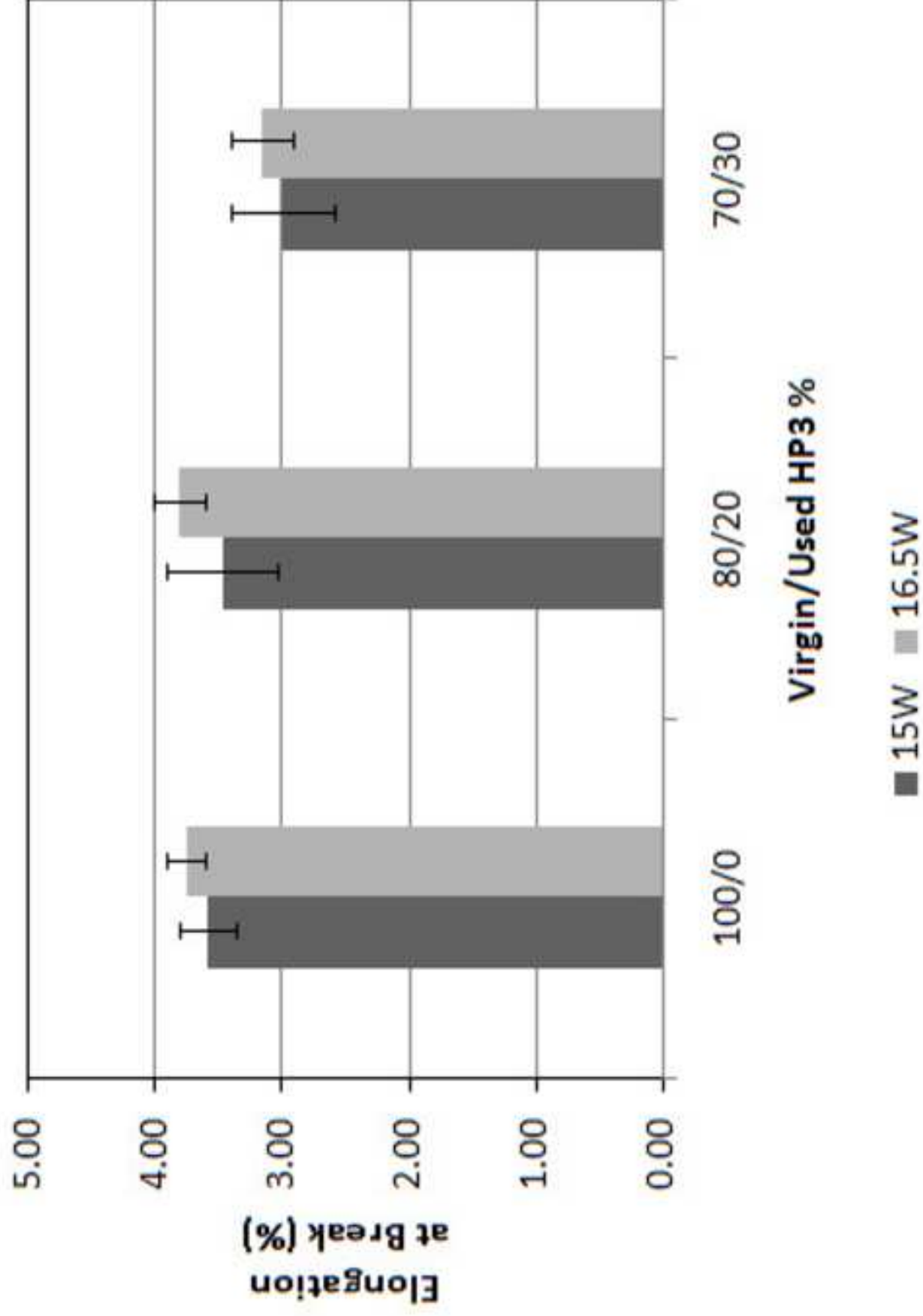


Figure 10
[Click here to download high resolution image](#)

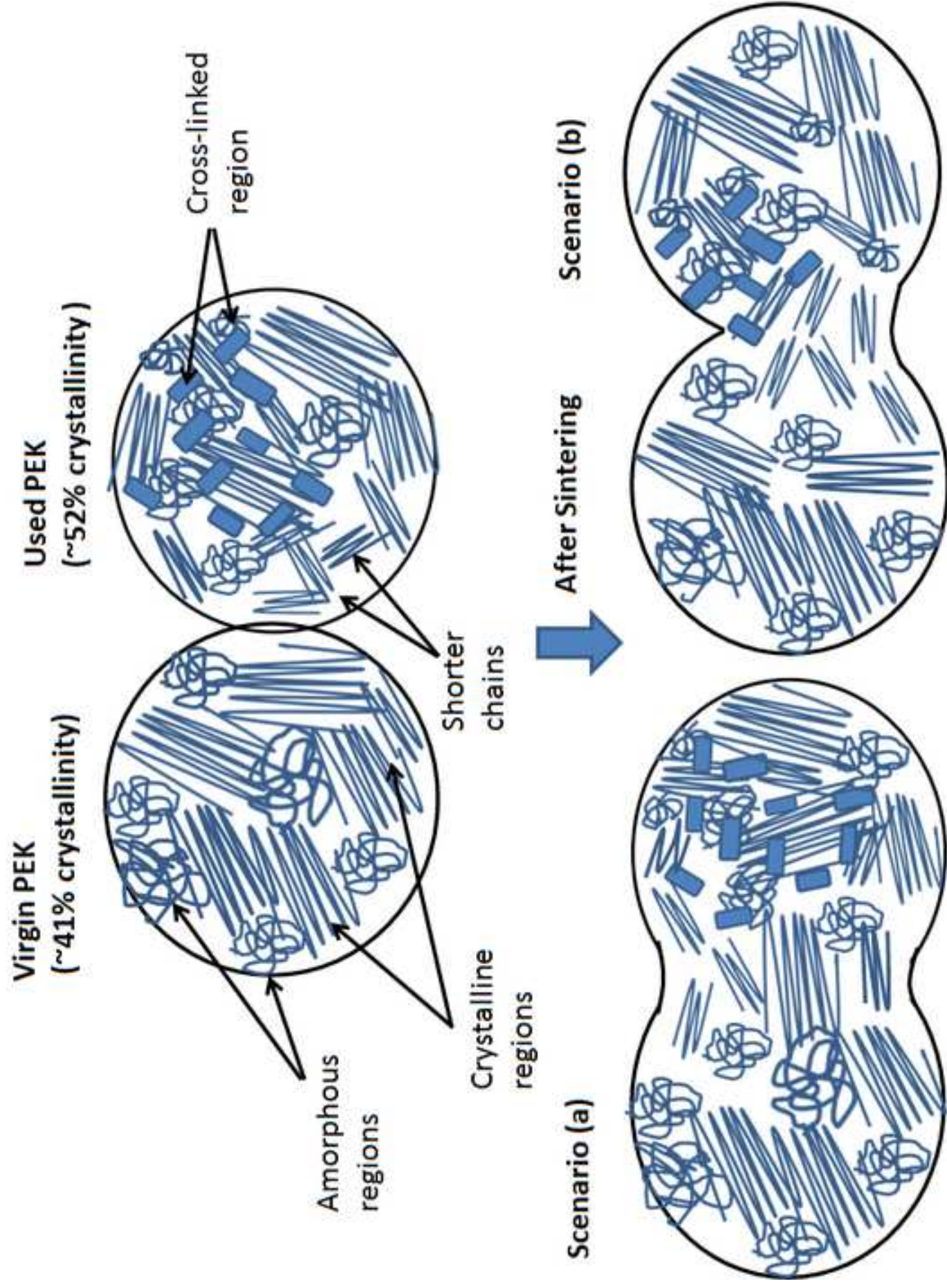


Figure 11
[Click here to download high resolution image](#)



Figure 12
[Click here to download high resolution image](#)



Figure 13
[Click here to download high resolution image](#)

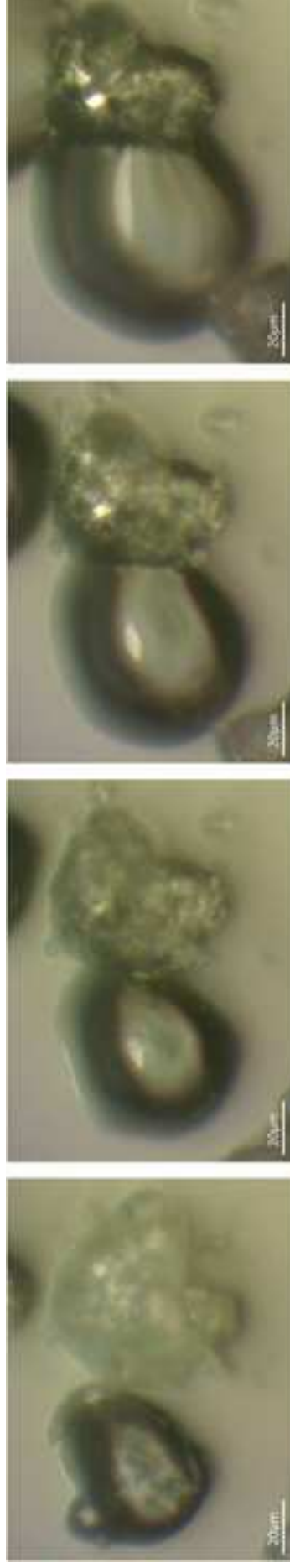
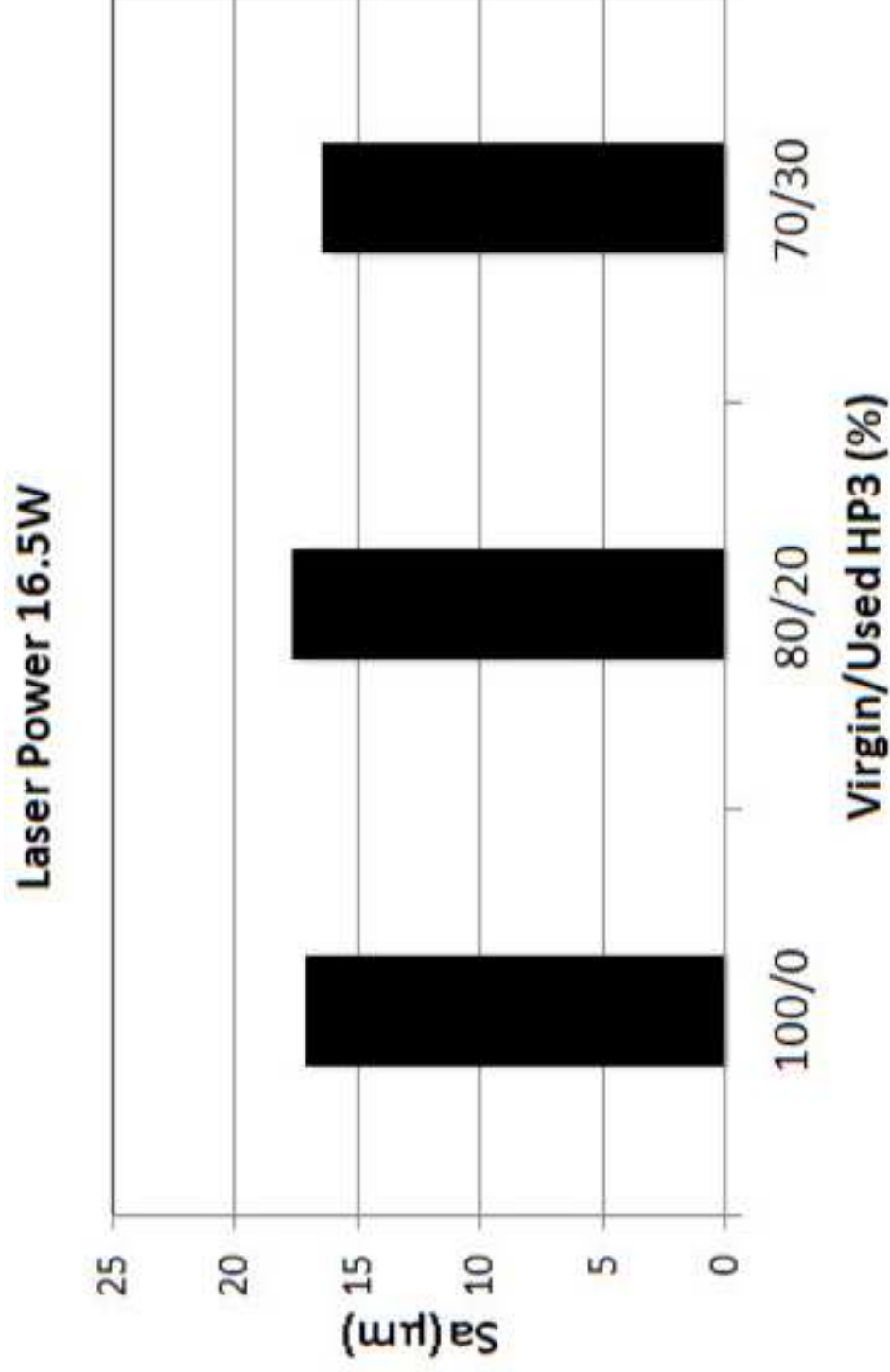


Figure 14a
[Click here to download high resolution image](#)



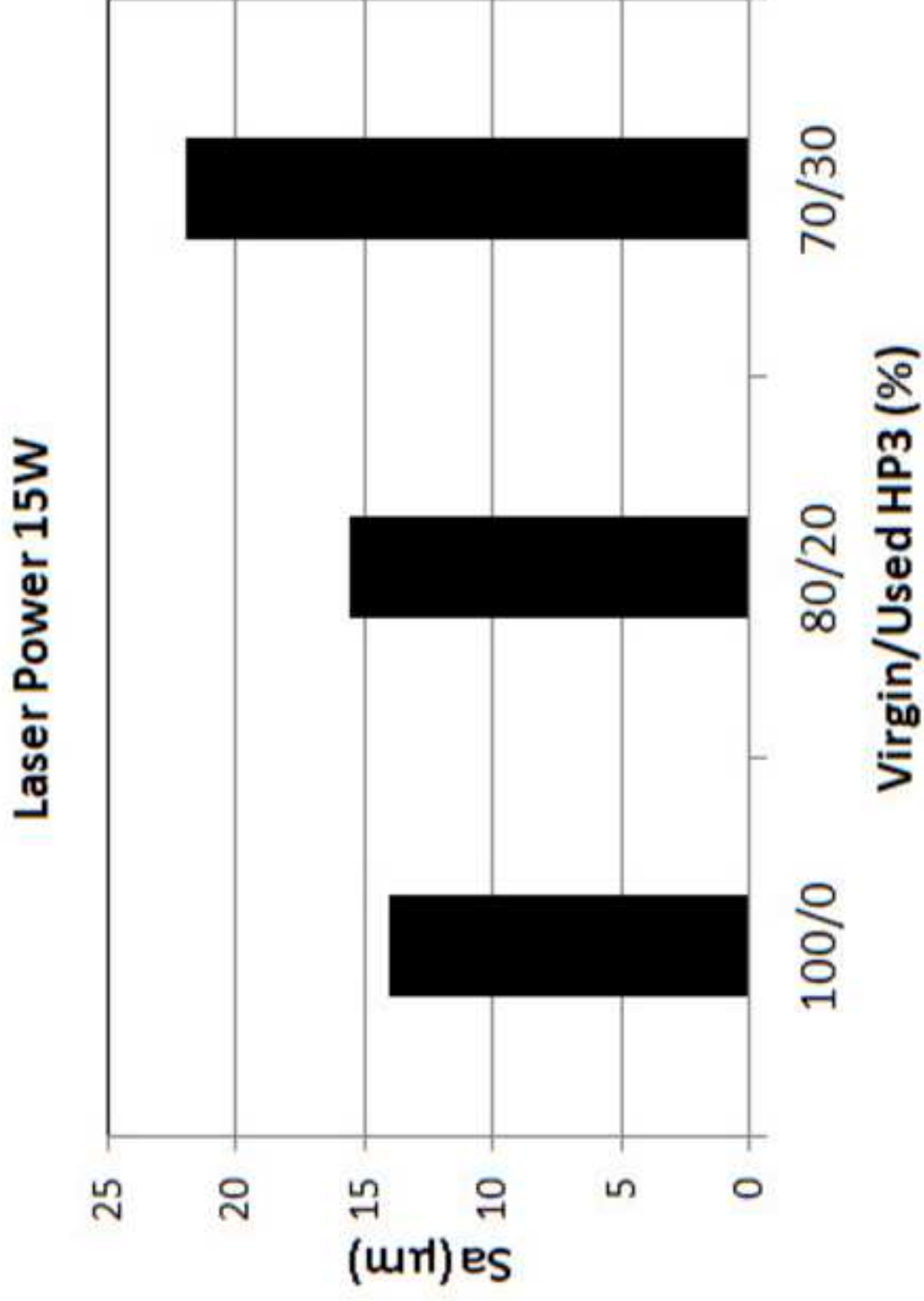


Figure 15a

[Click here to download high resolution image](#)

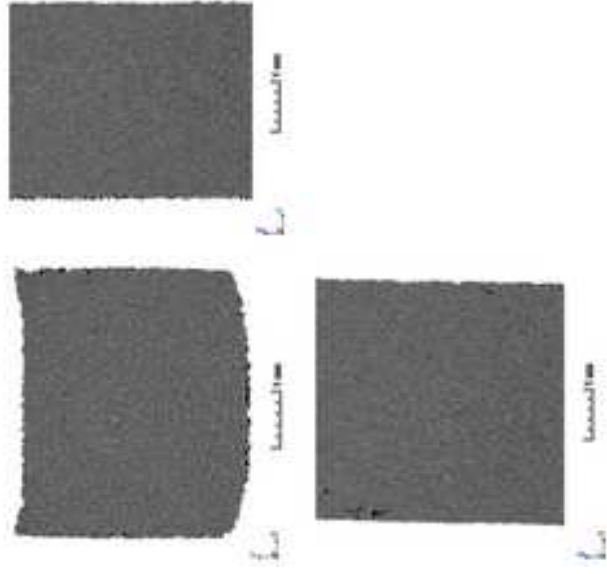


Figure 15b
[Click here to download high resolution image](#)

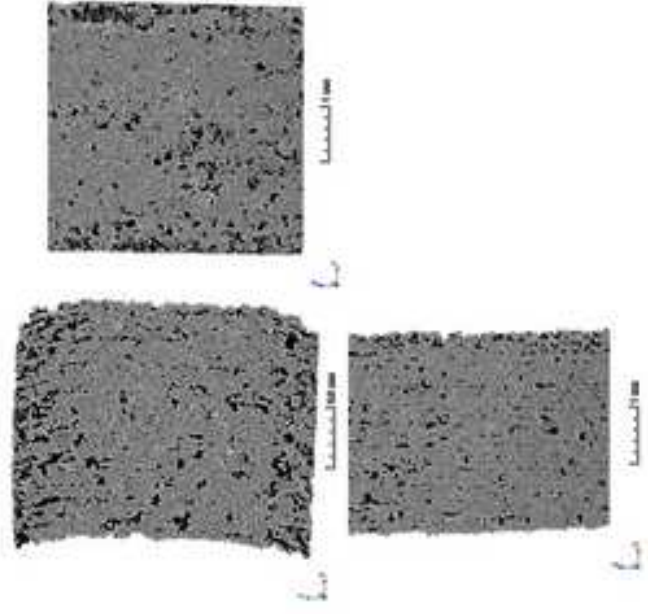


Figure 15c

[Click here to download high resolution image](#)

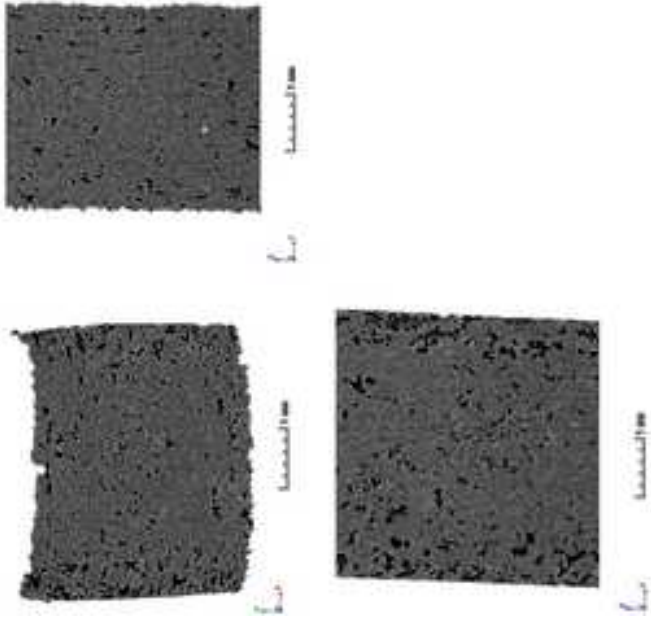


Figure 16
[Click here to download high resolution image](#)

